Coupled Ge/Si and Ge isotope ratios as geochemical tracers of seafloor hydrothermal systems: Case studies at Loihi Seamount and East Pacific Rise 9°50'N

Raphaelle Escoube, Olivier J. Rouxel, Katrina Edwards, Brian Glazer, Olivier François Xavier Donard

Geochimica et Cosmochimica Acta
October 2015, Vol. 167, Pages 93-112
http://dx.doi.org/10.1016/j.gca.2015.06.025
http://archimer.ifremer.fr/doc/00273/38403/

Coupled Ge/Si and Ge isotope ratios as geochemical tracers of seafloor hydrothermal systems: Case studies at Loihi Seamount and East Pacific Rise 9°50'N

Escoube Raphaelle [1, 2, 3], Rouxel Olivier [2, 4, *], Edwards Katrina [5], Glazer Brian [6], Donard Olivier F.X. [1]

[1] LCABIE, U. Pau et Pays de l'Adour, CNRS UMR 525, Hélioparc, 64053 Pau, France
[2] Université de Bretagne Occidentale, Institut Européen Universitaire de la Mer, Plouzané, France
[3] Dept. of Earth Sciences, University of Oxford, Oxford, UK
[4] IFREMER, Centre de Brest, Plouzané, France
[5] University of Southern California, USA
[6] Dept. of Oceanography, University of Hawaii, USA

* Corresponding author : Olivier Rouxel, email address : orouxel@ifremer.fr

Abstract :

Germanium (Ge) and Silicon (Si) exhibit similar geochemical behaviour in marine environments but are variably enriched in seafloor hydrothermal fluids relative to seawater. In this study, Ge isotope and Ge/Si ratio systematics were investigated in low temperature hydrothermal vents from Loihi Seamount (Pacific Ocean, 18°54'N, 155°15'W) and results were compared to high-temperature vents from the East Pacific Rise (EPR) at 9°50'N. Loihi offers the opportunity to understand contrasting Ge and Si behaviour in low temperature seafloor hydrothermal systems characterized by abundant Fe oxyhydroxide deposition at the seafloor. The results show that both Ge/Si and δ74/70Ge in hydrothermal fluids are fractionated relative to the basaltic host rocks. The enrichment in Ge vs. Si relative to fresh basalts, together with Ge isotope fractionation (Δ74/70Ge fluid-basalt up to 1.15 ‰ at EPR 9°50'N and 1.64 ‰ at Loihi) are best explained by the precipitation of minerals (e.g. quartz and Fe-sulfides) during higher temperature seawater-rock reactions in the subsurface. The study of Fe-rich hydrothermal deposits at Loihi, largely composed of Fe-oxyhydroxides, shows that Ge isotopes are also fractionated upon mineral precipitation at the seafloor. We obtained an average Ge isotope fractionation factor between Fe-oxyhydroxide (ferrihydrite) and dissolved Ge in the fluid of -2.0 ± 0.6 ‰ (2sd), and a maximum value of -3.6 ± 0.6 ‰ (2sd), which is consistent with recent theoretical and experimental studies. The study of a hydrothermal chimney at Bio 9 vent at EPR 9°50'N also demonstrates that Ge isotopes are fractionated by approximately -5.6 ± 0.6 ‰ (2sd) during precipitation of metal sulfides under hydrothermal conditions. Using combined Ge/Si and estimated Ge isotope signatures of Ge sinks and sources in seawater, we propose a preliminary oceanic budget of Ge which reveals that an important sink, referred as the "missing Ge sink", may correspond to Ge sequestration into authigenic Fe-oxyhydroxides in marine sediments. This study shows that combining Ge/Si and δ74/70Ge systematics provides a useful tool to trace hydrothermal Ge and Si sources in marine environments and to understand formation processes of seafloor hydrothermal deposits.

Keywords : Germanium isotope, Silica, Seafloor hydrothermal systems, Sulfides, Fe- oxyhydroxide

1. Introduction

Seafloor hydrothermal activity along mid-oceanic ridges is a fundamental process controlling global heat flux and chemical exchange between the oceanic crust and the oceans and provides a major source of dissolved silica to the ocean (e.g. Edmond et al., 1979; Stein and Stein, 1994; Elderfield and Schultz, 1996; Wheat et al., 2002; Wheat et al., 2004). Traditionally considered as a "pseudo-isotope' tracer for Silicon (Si), Ge/Si ratios in seawater and marine diatoms have been previously used to quantify Si fluxes to the oceans (Froelich and Andreae, 1981; Froelich et al., 1985a; Froelich et al., 1985b; Mortlock and Froelich, 1986; Froelich et al., 1989). In particular, it has been suggested that Ge/Si ratio in seawater could help to evaluate the relative proportion of hydrothermal vs. riverine input of silica to the global ocean (Mortlock and Froelich, 1986; Murnane and Stallard, 1988, 1990; Froelich et al., 1992; Mortlock et al., 1993; Elderfield and Schultz, 1996). Modern seawater is characterized by homogeneous Ge/Si ratios defined at about 0.7 µmol/mol. In contrast, hydrothermal vent fluids are characterized by higher Ge/Si values between 8 and 14 µmol/mol (Mortlock et al., 1993; Elderfield and Schultz, 1996), which is also higher than the average oceanic crust value defined at 2.2 µmol/mol (De Argollo and Schilling, 1978; Bernstein, 1985; Rouxel et al., 2006). The relative enrichment of Ge vs. Si in seafloor hydrothermal fluid and geothermal water has been generally considered to result from mineral-fluid interactions at depth, including the precipitation of Ge-poor secondary minerals, such as quartz and smectite (Arnorsson, 1984; Mortlock et al., 1993; Pokrovski and Schott, 1998; Evans and Derry, 2002). Low temperature weathering reactions may also affect Ge/Si ratios, considering the high affinity of Ge for iron oxyhydroxides, organic compounds and clay minerals (Bernstein, 1985; Kurtz et al., 2002).

Recently, Ge isotope ratios ($\delta^{74/70}$Ge) have been used as new geochemical tracers of Ge sources and behaviour in marine and hydrothermal environments (Rouxel et al., 2006; Siebert et al., 2006; Qi et al., 2011; Siebert et al., 2011; Escoube et al., 2012; Belissont et al., 2014). Based on the Ge isotope composition of modern marine biogenic silica, it has been suggested that the Ge isotopic composition of the ocean is enriched in heavy isotopes relative to the oceanic crust, by up to 2.5 ‰ (Rouxel et al., 2006, Escoube et al, 2012). Although the driving mechanisms controlling Ge isotopes in seawater are still unknown, establishing a preliminary balance of the Ge isotope composition in seawater requires: (1) placing boundaries on the Ge isotope composition of dissolved Ge that enters the ocean, e.g., through seafloor hydrothermal systems, and (2) investigating the fractionation of Ge isotopes during

Ge precipitation and sequestration, e.g., in clay, Fe-oxyhydroxides, and/or sulfides at the seafloor.

Here, we investigated hydrothermal vents from the Loihi Seamount (Pacific Ocean, 18°54'N, 155°15'W) that are characterized by distinct chemistry with high Fe and Si concentrations and low sulfide concentration, leading to the formation of extensive Fe-rich microbial mats and hydrothermal deposits at the seafloor (e.g. Emerson and Moyer, 2002; Glazer and Rouxel, 2009). Hence, the Loihi Seamount hydrothermal field provides an ideal site in which to study Ge-isotope systematics during hydrothermal alteration of volcanic rocks and Ge precipitation in Fe-rich deposits. We also investigated Ge isotope signatures of a well-studied high-temperature hydrothermal system from the East Pacific Rise (EPR) at 9˚50'N (e.g. Von Damm, 2004). The very young age of the lava flows along the axial summit trough of EPR at 9-10°N offers the opportunity to study Ge isotope systematics during the early stage of high-temperature hydrothermal venting and active formation of hydrothermal sulfide deposits.

The combined study of Ge/Si and Ge isotope ratios in both high- and low-temperature seafloor hydrothermal fluids and associated hydrothermal deposits allow a first estimate of the Ge isotope composition of the hydrothermal flux in the ocean and determine major processes affecting the fractionation of Ge isotopes between the oceanic crust and seawater. This approach is also required in order to apply Ge isotope chemistry as a useful paleo-oceanographic proxy in ancient marine sedimentary rocks.

2. Geological Setting

Loihi Seamount (Hawaii, 18°54'N, 155°15'W) is the youngest submarine volcano in the Hawaiian-Emperor Chain, rising ~4 km above the abyssal plain to a depth about 960 meters below sea level (mbsl) (**Fig. 1**). The vent fluids at Loihi are characterized as highly enriched in Fe, Mn, Si, CH_4 and CO_2 (Karl et al., 1988; Sedwick et al., 1992; Wheat et al., 2000; Glazer and Rouxel, 2009). The high CO_2 results in higher alkalinity and lower pH conditions (pH from 5.3 to 5.5) compared to many other low-temperature vents, inducing an important "chemical weathering" process of the volcanic rocks by carbonic acid. Although on occasion, aqueous sulfur species have been observed in Loihi's warmest vent fluids (~50^{o}C) using in-situ measurements (Glazer and Rouxel, 2009), Loihi vents lack H_2S enrichment, which contrasts with typical seafloor hydrothermal systems at mid-oceanic ridges (MOR). Another important feature of hydrothermal fluids at Loihi is that Mg concentrations remain

very close to background seawater, precluding the determination of “zero Mg” hydrothermal fluid end-members as is classically done for high-temperature mid-oceanic ridge vents (e.g. Von Damm et al., 1985).

It has been well recognized that Loihi vent fields support abundant and diverse prokaryotic populations, particularly among the Fe-oxidizing bacteria (FeOB). Likewise, biological oxidation in the Pele's Pit area at Loihi Seamount has been considered as responsible for ~60% of the total Fe-oxidation (Emerson and Moyer, 2002) and the formation of extensive seafloor Fe oxide deposits, referred to as microbial mats and modern analogues of umber deposits (Edwards et al., 2011). A variety of filamentous, non-filamentous, tubular, and branching particles have been recognized in the microbial mats (Karl et al., 1988; Emerson and Moyer, 2002; Fleming et al. 2013) with a mineralogy that includes ferrihydrite-like phases with short-range structural order (Toner et al., 2012). In such Fe-rich hydrothermal deposits, silica concentrations are also enriched, and Si occurs as either amorphous opal and/or Fe-rich smectite (De Carlo et al., 1983).

Our study involves a diverse set of samples, including hydrothermal fluids and Fe-rich deposits recovered during three cruises between 2006 and 2007 as part of the FeMO microbial observatory project (Glazer and Rouxel, 2009; Edwards et al., 2011). The samples are from three actively venting areas located at the summit of Loihi (**Fig. 1**): (1) Pele’s Pit crater which includes Spillway Area (Markers M34 and M38) and Hiolo Area (Markers M36 and M39); (2) Lohiau Area (Markers M2 and M5) located northern of Pele’s Pit crater; (3) Pohaku Area (Marker M57) located southern of Pele’s Pit. In general, vent fluids ranged in temperature from 21°C to 55°C with a pH between 5.6 and 7.3.

In order to compare with the low temperature hydrothermal systems at Loihi, we also reported Ge isotope signatures of high temperature hydrothermal systems from the East Pacific Rise (EPR) at 9˚50'N. This system is located on a fast-spreading ridge and is characterized by higher temperature (up to 350˚C) and lower pH (between 3.1 and 4.1) than Loihi Seamount. This high temperature venting site has been extensively investigated in previous studies (Haymon et al., 1993; Fornari et al., 1998; Shank et al., 1998; Von Damm, 2000; Von Damm, 2004; John et al., 2008; Rouxel et al., 2008). Hydrothermal fluid samples from EPR 9-10°N were recovered during cruise AT11-20, covering a range of vent temperatures from 200°C to 380°C which are associated with chalcopyrite, pyrite and sphalerite-rich chimneys. The hydrothermal field at EPR 9-10°N represents one of the youngest and most studied hydrothermal fields (e.g. Von Damm, 2004), thus permiting the

investigation of Ge isotope systematics in an environment where subsurface sulfide remobilization is likely limited, allowing the determination of representative Ge isotope composition for high temperature hydrothermal vents. Vent fluid chemistry and chimney mineralogy have been already reported elsewhere, including Fe, S and Zn isotopes (John et al., 2008; Rouxel et al., 2008).

3. Methods

During expeditions with ROV *Jason-II* (operated by the Woods Hole Oceanographic Institution), vent fields at Loihi seamount were widely surveyed in real-time using in situ voltammetry and temperature sensors (Glazer and Rouxel, 2009), and fluids were sampled using 750 mL titanium samplers ("Major" Ti- samplers) inserted directly into the vent orifice and triggered by a spring-loaded piston mechanism (Von Damm et al., 1985). Upon recovery on the ship, the samples were immediately filtered (0.2 μm filter pore size) and acidified to 0.06 M HCl. Detailed sample preparation and geochemical analysis procedures are reported in Glazer and Rouxel (2009). Briefly, fluid compositions (**Table 1**) were determined by ICP-MS (Thermo-Fisher Element 2) after 1:7 dilution with 0.28 M HNO_3 and appropriate standardization using matrix-matched standards. Seafloor Fe-rich particulate deposits were collected using the ROV *Jason-II* suction sampler (Edwards et al., 2011). The sampler is equipped with 5 L canisters that were flushed between each sampling operation to limit contamination between samples. Once retrieved, the canisters were sub-sampled for various chemical, mineralogical, and biological analyses. Particulates were separated from seawater by centrifugation, air-dried at 30°C, and powdered in agate mortar. Major and trace elements were analyzed at Activation Laboratories (Ancaster, Ontario) by ICP-AES and ICP-MS, respectively, after lithium metaborate/tetraborate fusion. Only selected major element concentrations (Si, Al, Fe and P) are reported in **Table 2** with an overall precision of 5% (2RSD) and detection limits below 0.01 wt%. Ge concentrations were obtained by isotope dilution and after chemical purification in the same split used for Ge isotope ratios measurements, as described below. Precision and detection limit for Ge concentrations analysis are better than 2 % (2RSD) and 0.01 μg/g respectively.

Ge isotope ratios and Ge concentrations were determined on MC-ICP-MS (Neptune, Thermo Scientific) at WHOI and IFREMER using the hydride generation technique described in Rouxel et al. (2006) and further modified in Escoube et al. (2012) using a ^{73}Ge:^{70}Ge double spike addition method. The analytical procedure is summarized below. The Fe-rich

hydrothermal deposits were first dissolved using concentrated distilled HNO_3. After complete evaporation at ~ 80 °C on a hot plate, the samples were further dissolved in 40 mL of 1 M HF solution (ultra-pure reagent grade) followed by an appropriate addition of Ge double spike (spike/natural ratio between 1 and 2). For sulfide minerals, samples were dissolved with concentrated distilled HNO_3 but not spiked, as described in Rouxel et al. (2006). For hydrothermal fluids, between 5 to 25 mL of sample solution was directly diluted to 40 mL with a 1 M HF concentration prior to adding Ge double spike and undertaking column separation. The sample solution in 1 M HF was then purified on an anion exchange chromatographic column (AG1-X8) as described in Rouxel et al. (2006). The total amounts of Ge processed through the entire chemical purification ranged from 40 ng for hydrothermal fluids to 200 ng for mineral deposits, yielding final Ge solution concentrations (in 0.28 M HNO_3) from 20 µg/g to 100 µg/g for isotopic analysis. The contribution of Ge from the whole procedural chemistry blank was measured for each batch of samples and has been found to be in all cases below 10 pg and indistinguishable from the instrumental blank determined by measuring pure 0.28 M HNO_3 solutions.

The MC-ICP-MS at WHOI and IFREMER was operated at low-mass resolution mode and ^{70}Ge, ^{72}Ge, ^{73}Ge and ^{74}Ge were measured on L2, C, H1, and H2 cups while ^{68}Zn, ^{69}Ga, ^{71}Ga and ^{77}Se were also monitored on L4, L3, L1 and H4 cups. The continuous flow hydride generation introduction system consisted of the CETAC HGX-200 directly connected to the ICP torch. Instrumental mass bias was corrected using two alternative techniques depending on sample types: (1) a double spike correction was performed for hydrothermal fluids and mineral samples from Loihi following a data reduction scheme similar to Siebert et al. (2006); (2) a sample-standard bracketing technique was applied to the analysis of sulfide minerals from EPR, following the approach of Rouxel et al. (2006).

The double spike was prepared from Ge metal spikes ^{73}Ge and ^{70}Ge purchased from Isoflex USA (Ge-70 #32-01-70-3259 and Ge-73 #32-01-73-1405). Each spike was dissolved separately and we obtained the following composition for the double spike: ^{74}Ge/^{70}Ge = 0.07614 ± 0.00010; ^{73}Ge/^{70}Ge = 0.60707 ± 0.00008; ^{72}Ge/^{70}Ge = 0.05626 ± 0.00008 (2sd uncertainties).

Ge isotope ratios were reported as $\delta^{74/70}$Ge values according to the following equation:

$$\delta^{74/70}Ge = \left(\frac{(^{74}Ge/^{70}Ge)_{sample}}{(^{74}Ge/^{70}Ge)_{NIST3120a}} - 1 \right) \times 1000 \qquad \textbf{(Eq. 1)}$$

Chemical compositions for hydrothermal fluids and deposits are reported in **Tables 1** to **3**. The NIST3120a (Lot #000411, 1000 µg/g) standard has been calibrated against previously used standards as reported in Escoube et al. (2012). Relative to NIST 3120a, the bulk crust, including both oceanic and continental crusts, has an average $\delta^{74/70}$Ge value of 0.59 ± 0.18 ‰ (2sd). The external 2sd uncertainties of the $\delta^{74/70}$Ge values were obtained through duplicated chemical purification and isotopic analysis of NIST 3120a standards and BHVO-2 obtained during the same analytical sessions.

A number of Geochemical Reference Materials (GRM) and standard solutions were already reported in Escoube et al. (2012). Average values for igneous rocks GRM (BHVO-2; BIR-1; BCR-1) yielded very limited variations, with $\delta^{74/70}$Ge = 0.56 ± 0.08 ‰. We also measured iron formation IF-G (IWG-GIT) and marine sediment GL-O (ANRT) and obtained $\delta^{74/70}$Ge values of 1.03 ± 0.10 ‰ (2sd) and 2.44 ± 0.14 ‰ (2sd) respectively.

4. Results

4.1. Hydrothermal fluids

Loihi vent fluids had a maximum temperature of 55°C and were all enriched in Fe, Mn, Si and Ge relative to background seawater (**Table 1**). As already discussed in previous studies (Karl et al., 1988; Sedwick et al., 1992; Wheat et al., 2000; Glazer and Rouxel, 2009), the positive correlation between Si, Fe and Mn concentrations reflects simple dilution with background seawater, either during fluid sampling or in the subsurface (**Fig. 2**).

Due to their relatively homogeneous Fe/Mn ratios ranging from 22 to 41 µmol/mol (average of 27 µmol/mol), Pele's Pit vents (Markers M34, M36, M38 and M39) were considered to be derived from the same fluid source at depth (hereafter referred to as fluid end-member) (Glazer and Rouxel, 2009). The lowest Fe/Mn ratios, associated with lower temperature vent fluids (below 25°C), were reported at the Northern part of Pele's Pit (i.e. Lohiau) and reflected subsurface Fe oxidation and precipitation (Glazer and Rouxel, 2009). Pohaku vents (M57), located south of Pele's Pit were also characterized by lower temperatures (28°C maximum) but with higher Fe/Mn ratios suggestive of subsurface interactions with volcanic rocks (Glazer and Rouxel, 2009).

Ge concentration in hydrothermal fluids at Loihi ranged from 10 to 180 nM, which is up to 3 orders of magnitude higher than seawater (e.g. Froelich et al., 1989; Mortlock and

Froelich, 1996). Si concentrations in Loihi vent fluids have been previously used as tracers of hydrothermal vent fluid dilution with seawater (Sedwick et al., 1992; Wheat et al., 2000; Glazer and Rouxel, 2009). Hence, the linear correlation between Ge and Si at Pele's Pit (markers M36, 39, 34, 38, 2, 5) with Ge/Si, at around 29.6 ± 1.6 µmol/mol, suggests that the overall variability of Ge concentration in vent fluids was mainly the result of fluid dilution with seawater (**Fig. 2a**). Pohaku vent fluids had distinctly lower Ge/Si ratios at around 8 µmol/mol confirming assumptions based on Fe/Mn ratios that different hydrothermal fluid end-members were venting at this site (Glazer and Rouxel, 2009).

High temperature hydrothermal fluids from EPR 9-10°N were also enriched in Ge vs. Si compared to source rocks (i.e. basalt with Ge/Si = 2.4 µmol/mol) with Ge/Si ratios between 3.7 and 8.5 µmol.mol^{-1}. Those values were lower than Pele's Pit vent fluids but consistent with other high temperature vent fluids from EPR 21°N and Juan de Fuca Ridge (Mortlock et al., 1993) (i.e. Ge/Si between 5 and 15 µmol/mol) (**Table 4**). In comparison, studies of Ge/Si in warm hydrothermal fluids from the ridge flank reported Ge/Si up to 60 µmol/mol, while cold formation fluids on ridge flanks yielded Ge/Si closer to basalt values (Wheat and McManus, 2008) (**Table 4**).

Pele's Pit vent fluids (markers M34, M36, M38 and M39) had $\delta^{74/70}$Ge values ranging from 1.2 to 2.2 ‰, averaging 1.68 ± 0.70 ‰ (2sd) and were thus systematically heavier than basaltic values defined at 0.56 ‰ (Rouxel et al., 2006; Siebert et al., 2011; Escoube et al., 2012) (**Table 1**, **Fig. 3**). Those $\delta^{74/70}$Ge values were, however, lighter than seawater ($\delta^{74/70}$Ge estimated at 3 ‰), which has been estimated at around 2.5 ‰ using deep-sea sponge values (Rouxel et al., 2006). Vent fluids from Lohiau and Pohaku areas had $\delta^{74/70}$Ge values between 0.95 to 1.23 ‰ and 0.61 to 0.74 ‰ respectively, and were thus lower than values obtained in Pele's Pit.

High temperature vent fluids from EPR 9-10°N yield $\delta^{74/70}$Ge values averaging 1.55 ± 0.36 ‰ (2sd, n=6) and were similar, albeit slightly lower, than the average $\delta^{74/70}$Ge value of low temperature hydrothermal fluids at Pele's Pit (**Tables 1** and **4**). Hence, despite their fundamental differences in temperature and chemical composition, high and low temperature hydrothermal vent fluids showed similar Ge isotope compositions characterized by a global enrichment in heavy Ge isotopes of about 1 ‰ relative to the basaltic source.

4.2. Seafloor hydrothermal deposits

At Loihi Seamount, hydrothermal deposits were composed essentially of Fe-oxyhydroxides and amorphous silica, which was reflected by the total Fe and Si concentrations up to 40 wt% and 15 wt%, respectively (**Table 2**). Significant amounts of goethite, Fe-montmorillonite and nontronite were reported in previous studies (De Carlo et al., 1983) but XRD analysis of our samples suggested only minor amounts of these clay minerals. Aluminium concentrations, reaching up to 2.3 wt% in some samples, were related to the addition of small amounts of volcanic glass fragments that had been entrained during mat sampling at the seafloor.

Ge concentrations in Loihi deposits range from 4.8 to 29.5 µg/g, with Ge/Si ratios from 37.5 to up to 189 µmol/mol (**Table 3**), which is one order of magnitude higher than for the associated hydrothermal fluids (Ge/Si at around 31 µmol/mol). Bulk Ge isotope compositions of Loihi Fe-rich deposits yield $\delta^{74/70}$Ge values between 0.16 and -0.98 ‰, lighted than basalt ($\delta^{74/70}$Ge = 0.56 ‰) and hydrothermal fluid values.

At EPR 9°50'N, hydrothermal deposits, including active and inactive chimneys, were composed of sulfide minerals such as chalcopyrite, pyrite, marcasite and sphalerite (Rouxel et al., 2008). Only Ge-enriched sulfides (i.e. sphalerite, pyrite, and marcasite) were analyzed for Ge isotope ratios (**Table 3**). Results showed systematically light $\delta^{74/70}$Ge values (down to -4.71 ‰), which are in marked contrast with the systematic heavy $\delta^{74/70}$Ge values of the hydrothermal fluid recovered from the same chimney at around 1.55 ‰.

5. Discussion

5.1. Coupled Ge/Si and Ge-isotope systematics in hydrothermal fluids

It has been already demonstrated that Ge/Si ratios in geothermal waters and hydrothermal fluids are systematically higher than Ge/Si ratios in source rocks (Arnorsson, 1984; Criaud and Fouillac, 1986; Evans and Derry, 2002). This enrichment may result from the preferential partitioning of Ge vs. Si in the fluid, considering the contrasting thermodynamic properties of aqueous $Ge(OH)_4$ and $Si(OH)_4$ in equilibrium with Ge-bearing silicates (Arnorsson, 1984; Pokrovski and Schott, 1998; Pokrovski et al., 2005). Experimental results show that Ge/Si ratio in hydrothermal fluid in equilibrium with quartz decreases with increasing temperature from 160 µmol/mol at 50°C, 43 µmol/mol at 250°C to about 30 µmol/mol at 400°C (Pokrovski and Schott, 1998; Evans and Derry, 2002).

Based on field data, Evans and Derry (2002) also proposed a model of progressive Si loss via precipitation of Ge-poor quartz (i.e. Rayleigh distillation) in order to explain the extreme increase of the Ge/Si ratio in cooled hydrothermal fluids. This model, requiring a high level of Si loss along a reaction path in order to produce observed Ge/Si ratios, is however not applicable to seafloor hydrothermal systems. The main reason is that measured Si concentrations of hydrothermal fluids, both at Loihi and EPR 9°50'N, are in equilibrium with quartz at the temperature and pressure (i.e. depth) corresponding of the base of the upflow zone at high temperature (>300°C) (Mottl, 1983; Von Damm et al., 1991; Sedwick et al., 1992). As suggested by Sedwick et al. (1992), the Si vs. T relationship at Loihi suggests saturation with quartz at high temperature (> 300°C), which suggests that the high Si concentrations (up to 4 mM) at Loihi result from the contribution of high-temperature fluid in the subsurface. Using a Si-T diagram, the same authors also suggest that the decrease of Si concentration in the fluid is only due to dilution during mixing with seawater and that no precipitation of Si occurs during the upflow and cooling of the hydrothermal fluids. At EPR 9°50'N, both Ge/Si (~ 8 μmol/mol) and Si concentrations (~ 20 mM) are also consistent with thermodynamic data, suggesting that equilibrium with quartz occurs in the reaction zone at temperatures between 350°C-400°C. Hence, it is unlikely that a significant amount of Si precipitated during fluid upflow. This is consistent with the general model that hydrothermal solutions rise adiabatically through the upflow zone and neither gain nor lose Si as they rise, in spite of the high degree of quartz supersaturation that results from the drop in pressure (Von Damm et al., 1991).

Here, we further evaluate whether both high Ge/Si ratios and heavy $\delta^{74/70}$Ge values of hydrothermal fluids compared to source rocks may be explained by mineral-fluid partitioning in the reaction zone (i.e. batch fractionation). Because Si concentration in high-temperature hydrothermal fluids is controlled by quartz solubility (VonDamm et al., 1991), higher Ge/Si ratios in hydrothermal fluids venting at the seafloor may be buffered by quartz in the reaction zone (Mortlock et al., 1993; Wheat and McManus, 2005). Considering that processes affecting Ge/Si ratios may also fractionate Ge isotope ratios, we propose a model linking Ge/Si ratios and Ge isotope compositions in hydrothermal fluid in equilibrium with quartz (or other silicates) in the reaction zone. In this case, we can estimate the Ge-isotope fractionation factors between quartz (or other silicates) and fluid using the following mass balance equation:

$$\delta^{74/70}Ge_{Basalt} = X_{Fluid} \times \delta^{74/70}Ge_{Fluid} + (1 - X_{Fluid}) \times \delta^{74/70}Ge_{Qz} \quad \textbf{(Eq. 2)}$$

Where $\delta^{74/70}Ge_{Basalt}$, $\delta^{74/70}Ge_{Fluid}$, and $\delta^{74/70}Ge_{Qz}$, the Ge isotopic composition of basalt, fluid and quartz respectively. X_{Fluid}, the fraction of Ge partitioned in the fluid can be estimated using Ge/Si relationships, such as:

$$X_{Fluid} = \frac{Ge/Si_{Basalt} - K_d \times Ge/Si_{Fluid}}{Ge/Si_{Basalt} \times (1 - K_d)} \quad \textbf{(Eq. 3)}$$

where K_d, the partition coefficient defined as the ratio of Ge/Si in quartz relative to the solution: $K_d = (Ge/Si)_{Qz}/(Ge/Si)_{Fluid}$

Using $\delta^{74/70}Ge_{Basalt}$ = 0.56 ‰, Ge/Si_{Basalt} = 2.20 µmol/mol (Escoube et al., 2012), K_d = 0.02 (Evans and Derry, 2002); and $\delta^{74/70}Ge_{Fluid}$ and Ge/Si_{Fluid} measured at Loihi, we obtained $\delta^{74/70}Ge_{Quartz}$ values of about -2.4 ‰ (i.e. $\Delta^{74/70}Ge_{Qz\text{-}fluid}$ at about -4.1 ‰). Similar $\delta^{74/70}Ge_{Quartz}$ values could be obtained at EPR using K_d = 0.12. Although those values are highly sensitive to the choice of K_d values (**Eq. 3**), the results suggest that quartz precipitation favours the light Ge isotopes, as already suggested by Rouxel et al. (2006) and Siebert et al. (2011). It is important to note that theoretical calculations by Li et al. (2009) predict an opposite fractionation factor for quartz, with $\Delta^{74/70}Ge_{Qz\text{-}Fluid}$ of ~0 ‰, 0.63 ‰ and 1.0 ‰ at 450°C, 100°C and 40°C respectively which is at odds with field studies. Hence, further work is required to experimentally determine the Ge isotope fractionation factor between silicate minerals and fluid at hydrothermal temperature (>350°C). This issue can be also addressed by the analyses of quartz veins in both high- and low-temperature altered basalts.

An additional possibility explaining heavier $\delta^{74/70}Ge$ values in vent fluids relative to source rocks may be related to differences of reactivity of Ge and Si towards sulfides in the reaction zone. In a growing number of studies (Li et al., 2009; Escoube et al., 2012; Belissont et al., 2014), it has been shown that Ge isotopes are significantly fractionated during Ge incorporation in sulfides. In particular, results reported in **Table 3** show that Ge isotope composition in hydrothermal sulfides at Bio 9" vent may be up to -6.05 ‰ (-5.6 ± 0.6 ‰, 2sd on average) lower than in associated fluids even at hydrothermal temperature (see section 5.4

and **Table 1**). It has been tentatively proposed by Escoube et al. (2012) that such large Ge isotope fractionation between sulfides and fluids may be related to the preferential substitution of Ge^{II} in sulfides. Hence, the increase of Ge/Si ratios and heavier $\delta^{74/70}$Ge values of seafloor hydrothermal fluids cannot be explained solely by sulfide precipitation. In addition, considering that both high- and low-temperature vent fluids have higher Ge/Si ratios and $\delta^{74/70}$Ge values, we do not favour the hypothesis that Ge sequestration in quartz during fluid upflow (i.e. Rayleigh distillation mechanism) is an effective mechanisms to affect Ge/Si and $\delta^{74/70}$Ge values. Therefore, we suggest that both quartz and sulfide precipitation in the reaction zone should act in conjunction to control both Ge/Si and Ge isotope signatures in seafloor hydrothermal fluid.

5.2. Importance of subsurface processes in affecting Ge geochemistry in hydrothermal fluids

Although all vents in the Pele's Pit hydrothermal field are likely fed by the same end-member fluid at depth, there was significant variability in Ge/Si, Fe/Mn and $\delta^{74/70}$Ge between vent sites or sampling periods. Since both Fe/Mn and Ge/Si ratios at Loihi are not affected by vent fluid mixing with seawater, it may be expected that vent fluids affected by subsurface mineral precipitation/dissolution processes could be distinguished using their Fe/Mn vs. Ge/Si relationships**.**

Hydrothermal fluids from marker M5 yield the most variable Ge/Si and Fe/Mn. In particular, Ge/Si range from 21 to 52 µmol/mol, being both the lowest and highest values found in Pele's Pit (**Table 1**). Although no clear systematics between Fe/Mn and Ge/Si ratios can be observed (**Fig. 2**), the close proximity of M5 relative to other Pele's Pit vents suggests similar end-member fluid values. Hence, the variable Ge/Si ratios and lower Fe/Mn ratios may be due to subsurface reactions during cooling of the fluids beneath the Fe-rich deposits. M5 also features the lowest $\delta^{74/70}$Ge values at Pele's Pit at 1.13 ± 0.25 ‰ on average (**Fig. 3, Table 1**). Since the M5 area lacks a well-defined outflow zone and is intensively covered by thick Fe-rich deposits (Glazer and Rouxel, 2009), it is possible that lower $\delta^{74/70}$Ge values associated with higher Ge/Si were due to Ge leaching from the surrounding seafloor hydrothermal deposits having lighter $\delta^{74/70}$Ge values and higher Fe/Mn and Ge/Si ratios.

Hydrothermal fluids from marker M57 yielded lower Ge/Si ratios, averaging 7.9 ± 1.3 µmol/mol, and higher Fe/Mn ratios, which likely reflect a different pathway of hydrothermal

fluids relative to Pele's Pit vents (**Table 1).** M57 was also characterized by lighter $\delta^{74/70}$Ge values compared to Pele's Pit fluids, bringing the isotope composition closer to basalt values (**Fig. 3**). Lower Fe/Mn ratios at M57 have already been interpreted as reflecting a stronger interaction with basalt during fluid circulation (Glazer and Rouxel, 2009) due to longer residence time of the fluid in subsurface environments (Wheat et al., 2000). More intense weathering (i.e. near congruent dissolution due to CO_2-induced alteration) provides an adequate explanation for lower Ge/Si and $\delta^{74/70}$Ge values that are intermediate between Pele's Pit vents and basalts.

5.3. The geochemistry of Ge isotopes in Fe-rich hydrothermal deposits at Loihi

The Fe-rich hydrothermal deposits at Loihi are related to the formation of extensive Fe-rich microbial mats formed by the oxidation of hydrothermally-derived Fe at or below the seafloor (De Carlo et al., 1983; Karl et al., 1988). Iron precipitation is considered to result mainly from microbial oxidation mediated by neutrophilic *Zetaproteobacteria*, which have been estimated to contribute to ~60% of total Fe oxidation of the hydrothermal fluids circulating through the microbial mats (Emerson and Moyer, 2002; Emerson et al., 2007). Reactive oxyanions in vent fluids and seawater, such as phosphate and germanic acid (H_4GeO_4) are readily adsorbed onto goethite and ferrihydrite and coprecipitate with amorphous Fe oxyhydroxides particulates. P and Ge are therefore significantly enriched in the Fe-rich deposits at Loihi Seamount (**Table 2)**. Upon oxidative precipitation of Fe, amorphous silica from the hydrothermal fluid may also precipitate. It is important to note that Fe sulfide minerals are absent at Loihi (Toner et al., 2012), mainly because of the lack of H_2S in the hydrothermal fluids (Glazer and Rouxel, 2009). It should be also noted that the low organic C content of the mats, as well as the development of microaeorophilic conditions, preclude active microbial sulfate and iron reduction, which is generally observed in reducing marine sediments. The preferential enrichment of Ge vs. Si in Fe-rich mineral deposits has been reported in numerous studies and interpreted as resulting from the strong affinity of Ge toward Fe oxyhydroxides (Bernstein, 1985; Kurtz et al., 2002; Pokrovsky et al., 2006; Pokrovsky et al., 2014). Hence, Ge in the Fe-rich hydrothermal deposits is potentially hosted in three pools (1) Fe oxyhydroxides, (2) amorphous silica, and (3) volcanic debris.

The Fe-rich deposits at Loihi Seamount have low $\delta^{74/70}$Ge values from 0.16 down to -0.98 ‰ (**Table 2**), which corresponds to a maximum apparent $\Delta^{74/70}Ge_{deposit\text{-}fluid}$ of -2.81 ‰

(**Fig. 3**). The largest fractionation factor between fluid and Fe-rich deposit is broadly consistent with experimental data for Ge coprecipitation with amorphous iron oxyhydroxide up to -4.4 ‰ (Pokrovsky et al., 2014). However, since $\delta^{74/70}$Ge signatures in microbial mats are muted by the relative proportion of Ge hosted in amorphous silica, basalt fragments or Fe oxyhydroxides, the $\delta^{74/70}$Ge values of the pure Fe oxyhydroxide end-member should be calculated using the following mass balance equation:

$$\delta^{74}Ge_{deposit} = \mathrm{XGe_{Bas}} \times \delta^{74}Ge_{\mathrm{Bas}} + \mathrm{XGe_{Amo}} \times \delta^{74}Ge_{\mathrm{Amo}} + XGe_{\mathrm{FeOOH}} \times \delta^{74}Ge_{\mathrm{FeOOH}} \quad \textbf{(Eq. 4)}$$

with XGe, the fraction of mass Ge in each component (Bas: basalt; Amo: amorphous silica; FeOOH: Fe oxyhydroxide).

The fraction of Ge in basalt (XGe_{Bas}) can be calculated using Al concentration, if we consider that Al is only hosted in the basalt component:

$$XGe_{Bas} = \left(\frac{Al}{Ge}\right)_{measured} \times \left(\frac{Si}{Al}\right)_{Bas} \times \left(\frac{Ge}{Si}\right)_{Bas} \quad \textbf{(Eq. 5)}$$

With $Al/Ge_{measured}$ the measured ratio in the mat (in g/g); Si/Al_{Bas} the average ratio previously reported for basalts at Loihi (Frey and Clague, 1983) equal to 2.95; and Ge/Si_{Bas} the average ratio reported for basaltic rocks around 5.7 $\mu g.g^{-1}$ (i.e. 2.2 µmol.mol-1, De Argollo and Schilling, 1978; Halicz, 1985; Kurtz et al., 2002). The Ge isotope composition of the basalt pool is also taken from the average crustal (i.e., oceanic and continental crusts) values defined at $\delta^{74/70}Ge_{Bas}$ = 0.56 ‰ (Rouxel et al., 2006; Escoube et al., 2012).

The fraction of Ge in amorphous silica (XGe_{Amo}) can be also estimated, according to the equation:

$$XGe_{Amo} = \frac{K_d}{Ge_{measured}} * \left(\frac{Ge}{Si}\right)_{fluid} \times \left[Si_{measured} - Al_{measured}\left(\frac{Si}{Al}\right)_{Bas}\right] \quad \textbf{(Eq. 6)}$$

Where $K_d = (Ge/Si)_{Amo}/(Ge/Si)_{Fluid}$. K_d is potentially equal to unity (i.e. no fractionation) as is the case for biogenic opal precipitation (Lewin, 1966; Azam et al., 1974; Azam and Volcani, 1981; Froelich and Andreae, 1981; Murnane and Stallard, 1988; Froelich et al., 1992; Bareille et al., 1998) or lower than unity at about 0.02 as is the case for quartz

precipitation (Evans and Derry, 2002). Note that the amount of Si derived from direct fluid precipitation is corrected for basalt contributions in **Eq. 6**.

The Ge isotope composition of the amorphous silica pool is, at a first approximation, taken to be equal to the composition of the hydrothermal fluid, which is consistent with biogenic opal precipitation which appears to not fractionate Ge isotope significantly (Mantoura, 2006). However, this issue will need to be re-evaluated when experimental studies become available. Finally, the fraction of Ge in FeOOH is determined as the residual Ge pool such that:

$$XGe_{FeOOH} = 1 - XGe_{Bas} - XGe_{Amo} \qquad (\textbf{Eq. 7})$$

Where XGe_{Bas} and XGe_{Amo} are determined using Eq. 5 and Eq. 6 respectively. This approach allows the Ge isotope composition of the FeOOH pool to be calculated using equation (**Eq. 4**) for all samples (**Table 4**). In order to take into account the measurements uncertainties of input values in equations (**Eq. 4-7**), we propagated errors using a Monte Carlo simulation at 95% confidence level. For this stochastic simulation, we propagated uncertainties for both $\delta^{74/70}$Ge and Ge/Si values of the hydrothermal vent fluids. We also propagated uncertainties in K_d values, taken at 0.5 ± 0.4 which encompasses all K_d values expected for amorphous silica or silicate precipitation. Results presented in **Table 5** show that approximately 90% of total Ge is associated with iron oxyhydroxides (i.e. XGe_{FeOOH}); except for samples with significant Si enrichments (XGe_{amo} up to 27%). For all samples the proportion of detrital (i.e. basaltic) Ge is less than 5%. It is evident that, for samples having the highest Si enrichment (e.g. J2-308-SS2), the amount of Ge hosted in amorphous silica depends highly on the value of the partition coefficient K_d. For samples with more than 90% of Ge hosted in Fe-oxyhydroxides, the calculated $\delta^{74/70}Ge_{FeOOH}$ values are shifted to lighter values by only 0.25 ‰ relative to bulk $\delta^{74/70}$Ge values, and therefore very similar within uncertainty.

Using calculated $\delta^{74/70}Ge_{FeOOH}$ values, it is possible to determine, for each sample, the apparent Ge isotope fractionation factor between the source fluid and precipitated Fe oxyhydroxide ($\Delta^{74/70}Ge_{FeOOH\text{-}fluid}$). The results (**Table 5**) show a range of $\Delta^{74/70}Ge_{FeOOH\text{-}fluid}$ values, from -3.6 ± 0.9 ‰ (2sd) at M34 to -0.9 ± 0.2 ‰ (2sd) at M57. Excluding those 2 extreme values, $\Delta^{74/70}Ge_{FeOOH\text{-}fluid}$ is rather homogeneous for the Pele's Pit area, with an

average of -2.0 ± 0.6 ‰ (2sd). In comparison, Pohaku shows smaller $\Delta^{74/70}Ge_{FeOOH-\ fluid}$ at -0.9 ± 0.2 ‰ (2sd). By comparison, Pokrovsky et al. (2014) determined the Ge isotope fractionation factor $\alpha_{FeOOH-Fluid}$ at about 0.9956 (i.e. $\Delta^{74/70}Ge_{FeOOH-fluid}$= -4.4 ‰) at room temperature demonstrating that light Ge isotopes are preferentially sequestrated into Fe-oxyhydroxides.

Using first-principles density functional theory, Li and Liu (2010) calculated Ge isotope fractionation factors for the adsorption of aqueous Ge species onto Fe(III)-oxyhydroxide surfaces. Calculated fractionation factors ranged from -1.5 to -1.9 ‰ at temperatures between 20°C and 50°C and were almost insensitive to pH. Hence, our results are consistent with both previous experimental and theoretical studies. Our estimate of $\Delta^{74/70}Ge_{FeOOH-fluid}$ at -2.0 ± 0.6 ‰ (2sd) is, however, smaller than experimental studies by Pokrovsky et al. (2014), which may be explained by a different coordination configuration of adsorbed Ge as well as competition with others chemical species such as silica. For example, the different (i.e. lower) fractionation factor during Ge sorption at Pohaku may be related to the structure of Fe-oxyhydroxide particles that are distinct from the Pele's Pit area (Haddad et al., in prep).

It is also possible that Ge sorption onto Fe-rich deposits at Loihi does not proceed in a completely open system, i.e. when the rate of Ge precipitation is faster than the supply of Ge from hydrothermal fluids. In this case, the apparent fractionation factor $\Delta^{74/70}Ge_{FeOOH-fluid}$ is related to the amount (f_{ads}) of Ge adsorbed onto Fe oxyhydroxide using the equation:

$$\Delta^{74/70}Ge_{FeOOH-\ fluid} = (1-f_{ads}) \times 1000 \ln (\alpha_{FeOOH-\ fluid}) \qquad \textbf{(Eq. 8)}$$

with $\alpha_{FeOOH-\ fluid}$ being the equilibrium fractionation factor between Ge adsorbed onto Fe oxyhydroxide and Ge in solution. Using $\alpha_{sol-liq}$ of about 0.996 as determined by Pokrovsky et al. (2014), we can calculate that $\Delta^{74/70}Ge_{FeOOH-fluid}$ of about -2 ‰ corresponds to more than 30% of Ge from the hydrothermal fluid that is precipitated within Fe-rich deposits (**Table 5**). In the case of Pohaku (M57) showing a $\Delta^{74/70}Ge_{FeOOH-fluid}$ of -0.9 ‰, the amount of Ge precipitation may increase to up to 70% (**Table 5**). The fact that more than 30% of Ge from the hydrothermal fluid may be precipitated at the seafloor suggests that Fe-rich deposits provide a relatively efficient trapping of reactive elements coming from the diffuse vent fluids. This finding contrasts with high-temperature hydrothermal chimneys that behave as an

open system relative to vent fluids; i.e., only a small fraction of elements is trapped within the chimney wall (Tivey, 1995).

5.4. Preliminary estimation of Ge fractionation in hydrothermal sulfide deposits

Through a combined approach using hydrothermal sulfide deposits and associated fluids, we can estimate the apparent Ge isotope fractionation factor ($\Delta^{74/70}Ge_{sulfide\text{-}fluid}$) between Fe-Zn sulfides (sphalerite +/- pyrite) and the fluids. Isotopically light $\delta^{74/70}Ge$ values of hydrothermal sulfide deposits at EPR 9-10°N (down to -4.71 ‰, **Table 3**) together with heavy composition of the hydrothermal fluids (average 1.55 ± 0.36 ‰, 2sd) allows us to estimate $\Delta^{74/70}Ge_{sulfide\text{-}fluid}$ values ranging from -5.17 to -6.28 ‰ with an average of -5.6 ± 0.6 ‰ (2sd).

Using quantum chemistry calculations, Li et al. (2009) determined $\Delta^{74/70}Ge_{sulfide\text{-}Ge(OH)4}$ at 25°C between -12.2 to -11.4 ‰ depending on Ge valence state and coordination (i.e. $Ge^{II}S_4Zn_2^{2-}$ and $Ge^{IV}S_4Zn_2^{0}$ sulfide species respectively). At Bio9 vent, the precipitation temperature of sphalerite along the chimney wall is generally below 250°C (Rouxel et al., 2008). Using the equation $\Delta^{74/70}Ge_{sulfide\text{-}fluid}=A*10^6/(T^2)+B$ and using the reduced isotope partition function ratio reported by Li et al. (2009), we estimate $\Delta^{74/70}Ge_{sulfide\text{-}fluid}$ at 250°C for $Ge^{II}S_4Zn_2^{2-}$ and $Ge^{IV}S_4Zn_2^{0}$ species (i.e. considering A = -1.083 and -1.012 respectively and B = 0 as a first approximation). Using this approach, the estimated theoretical $\Delta^{74/70}Ge_{sulfide\text{-}fluid}$ fractionation factors range from -3.97 to -3.71 ‰, which is consistent with the observed Ge isotope fractionation factors between hydrothermal fluids and sulfide minerals at Bio9 vent. We notice that differences in Ge redox state or coordination among different sulfide compounds do not drastically change isotope fractionation factors. In contrast, differences of Ge bonding environments such as found in Ge-S or Ge-O compounds appear to drive the largest isotope fractionation (Li et al., 2009).

5.5. Preliminary Ge-isotope mass balance in seawater

The average Ge/Si ratio in the global ocean is about 0.7 µmol/mol (Froelich and Andreae, 1981) which is significantly lower than the Ge/Si in basaltic rocks of 2.6 ± 0.3 $x10^{-6}$ µmol/mol (DeArgollo and Schilling, 1978). Because the two dominant Si and Ge sources to the ocean carry very different Ge/Si signatures, with $(Ge/Si)_{rivers}$ ~ 0.4 µmol/mol (Mortlock and

Froelich, 1987) and $(Ge/Si)_{hydrothermal}$ ~ 8-14 μmol/mol (Mortlock et al., 1993), it has been proposed that the Ge/Si ratio buried in biogenic siliceous tests on the seafloor reflects the present and past source strength of the river fluxes relative to hydrothermal fluxes (Elderfield and Schultz, 1996; Froelich et al., 1992; Murnane and Stallard, 1988). However, the use of Ge/Si as a paleoceanographic tool remains uncertain as the Ge mass balance in the modern ocean is not well understood. Assuming steady state, the contemporary input fluxes from continents and hydrothermal sources require Ge removal with a Ge/Si ratio of 1.6 μmol/mol, which is significantly greater than the observed opal burial ratio of 0.7 μmol/mol (Elderfield and Schultz, 1996). Identification and quantification of the so-called "missing Ge sink" has received great interest in the past decade and it is now proposed that Ge may be removed from the ocean in iron-rich reducing sediments of continental margins independently of Si (Hammond et al., 2000; King et al., 2000; McManus et al., 2003). This sink corresponds to about 55 ± 9% of Ge within opal released by dissolution (Hammond et al., 2000). Considering the potential of Ge isotopes to fractionate during marine sediment diagenesis, for example during Ge precipitation with authigenic minerals, Ge isotope systematics should be a powerful tool to further constrain the missing sink through the establishment of a mass balance of Ge isotopes in the oceans.

First, it is important to note that the Ge isotope composition of modern seawater is poorly known. Using the Ge isotope ratios of marine biogenic opal such as sponges, Rouxel et al. (2006) previously suggested that seawater is enriched in heavy Ge isotopes relative to the continental crust by up to 2.5 ‰. However, an unpublished study of the Ge isotope composition of seawater (Baronas et al., 2014) showed that seawater $\delta^{74/70}$Ge values range from 3.9 to 3.4 ‰, which is about 3 ‰ heavier than oceanic and continental crust values. The later study confirms a previous report of $\delta^{74/70}$Ge values of marine diatoms from Holocene sediments at around 3.3 ‰ (Mantoura, 2006). Hence, a value of 3.0 ±0.6 ‰ is probably a good estimate of modern seawater $\delta^{74/70}$Ge values considering the current knowledge.

Secondly, preliminary investigations of Ge isotope fractionation by marine diatoms revealed that biological uptake of Ge does not fractionate $\delta^{74/70}$Ge values, in contrast to Si isotopes (Mantoura, 2006). Hence, it can be suggested that seawater $\delta^{74/70}$Ge values are probably not modified by the biogenic opal sink – and therefore by marine productivity.

With these conditions and considering steady state, the heavy Ge isotope composition of seawater requires either: (1) heavier $\delta^{74/70}$Ge values for the global Ge input (i.e. rivers and

hydrothermal vents combined) relative to the continental crust; or (2) a Ge output via the "missing Ge-sink" (e.g. authigenic phases in marine sediments) characterized by lower than crustal $\delta^{74/70}$Ge values; or (3) a combination of both.

In order to address these issues, we establish a preliminary mass balance of Ge in seawater, using a one box ocean model based on Ge/Si, $\delta^{74/70}$Ge and the marine Ge source and sink fluxes (**Table 6**). At steady state, the sum of input fluxes and output fluxes of Ge to the ocean are equal:

$$F_{River} + F_{Atmospheric} + F_{Hydrothermal} + F_{Low-TBasalt} = F_{Opal} + F_{Non-Opal} \quad \textbf{(Eq. 9)}$$

With, F, the flux of Ge of each of the inputs and outputs determined based on their Ge/Si ratios and Si fluxes (From Hammond et al., 2000; King et al., 2000; McManus et al., 2003). Considering steady-state conditions, the mass balance of Ge isotopes in seawater is defined as:

$$\sum_{Source}\left(F \times \delta^{74}Ge\right) = \sum_{Sink}\left(F \times \delta^{74}Ge\right) \quad \textbf{(Eq. 10)}$$

In order to determine the Ge isotope signature of the missing, non-opal Ge sink, we resolve **Eq. 9** and **10** using estimated $\delta^{74/70}$Ge and Ge/Si values of other Ge sinks and sources (**Table 6**), such as:

(1) $\delta^{74/70}$Ge value of atmospheric deposition (i.e. aeolian particles) has been estimated to be identical to crustal values, with $\delta^{74/70}$Ge = 0.56 ±0.20 ‰ as estimated by Escoube et al. (2012). Si and Ge fluxes from atmospheric deposition were taken from the estimation of King et al. (2000).

(2) Ridge flanks Ge and Si fluxes, including the sum of warm (40–75°C) hydrothermal systems and low-temperature seafloor basalt weathering were taken from Wheat and McManus (2005). Because of the large range of Ge/Si ratios in warm hydrothermal fluids from ridge flanks, we applied an uncertainty of 50% to the estimated fluxes (**Table 6**). $\delta^{74/70}$Ge of ridge flank fluxes is also considered similar the average value obtained at Loihi ($\delta^{74/70}$Ge = 1.2 ±0.5 ‰). Despite the relatively large uncertainties, the ridge flank Ge fluxes have a minor influence on global Ge oceanic cycle due to their small contribution representing less than 10% of the total Ge input.

(3) Si and Ge fluxes from rivers were taken from the estimation of King et al. (2000). $\delta^{74/70}$Ge values of rivers are however presently unknown. As a first approximation, we consider the riverine flux to have a similar $\delta^{74/70}$Ge value as the average crustal value. Ge/Si in rivers are well known to be fractionated relative to bulk earth (with a ratio around 0.58 µmol/mol versus 1.3 µmol/mol for the crust, Mortlock and Froelich, 1987). Therefore, the Ge isotope composition of rivers is likely to be fractionated relative to the crust due to Ge sorption on clay or oxide minerals, as previously observed by Kurtz et al. (2002) and Scribner et al. (2006). Because rivers represent 37% of the global input of Ge, it is clear that a better constraint on the riverine flux is important for establishing a reliable isotope mass balance in seawater. In order to address this issue, we performed a simple sensitivity test by running our mass balance model using $\delta^{74/70}$Ge of rivers identical to either seawater values or average crust values (**Table 6**).

(4) The $\delta^{74/70}$Ge value of the high-temperature (HT) hydrothermal flux is estimated as at 1.55 ±0.36 ‰ based on average values obtained from high-temperature vent fluids from EPR. The Ge/Si of the HT hydrothermal flux is determined at 11 ±3 µmol/mol based on the compilation of Ge/Si values for high-temperature hydrothermal vents presented in **Table 2**. It should also be recognized that Ge (and Si) fluxes from acidic volcanic island arcs, which represent about 10% of the hydrothermal flux (Baker et al., 2008), and back arc spreading centers are poorly known. Considering the contrasting chemical composition of hydrothermal fluids in such settings, including high volatile contents (e.g. SO_2) and low pH values (Resing et al., 2007; Butterfield et al., 2011; Craddock et al., 2010), it is possible that they contribute differently to Ge and Si fluxes.

(5) The $\delta^{74/70}$Ge values of the opal sink are considered identical to seawater values as demonstrated in previous studies showing a lack of Ge/Si and Ge-isotope fractionation during diatom uptake (Shemesh et al., 1989; Bareille et al., 1998; Mantoura, 2006). Mantoura (2006) reported $\delta^{74/70}$Ge values at around 3.3 ‰ for diatom opal from Holocene sediments. These results, together with the lack of Ge isotope fractionation observed during Ge uptake by cultured diatoms (Mantoura 2006) and preliminary Ge isotope measurement of seawater (Baronas et al., 2014) suggest that seawater is enriched in heavy Ge isotopes. In this model, we used a $\delta^{74/70}$Ge value of 3.0 ±0.6 ‰ for seawater.

(6) The removal of elements in hydrothermal plume through adsorption onto FeOOH-rich particles is well recognized for seawater oxyanions such as V, As and P (Feely et al.,

1990, 1991) but is probably negligible for Ge. In particular, it has been demonstrated that $Ge/^{3}He$ ratios of the dispersing hydrothermal plume remain close to high-temperature hydrothermal vent end-member values, suggesting a near conservative behaviour of Ge during seawater-hydrothermal fluid mixing (Mortlock et al., 1993).

We ran our box model using the parameters defined in **Table 6** and by applying an error propagation scheme (i.e. Monte Carlo simulation). We solved simultaneously **Eq. 9-10** in order to estimate the $\delta^{74/70}$Ge value of the missing, non-opal Ge sink for the cases of (i) riverine input at crustal values and (ii) riverine input identical to seawater values. In the first case, we determined the $\delta^{74/70}$Ge value of the non-opal Ge sink to be -0.6 ± 0.4 ‰, which is about 3.6 ‰ lighter than seawater. In the second case, we obtained heavier $\delta^{74/70}$Ge value at 0.9 ± 0.3 ‰ for the missing Ge sink, which is about 2.1 ‰ lighter than seawater. These values, albeit different, correspond to the expected isotope fractionation produced by Ge adsorption onto Fe-oxyhydroxide estimated at 2.0 ‰ on average (this study) and up to 4.4 ‰ as determined by Pokrovsky et al. (2014). It is however important to note that both the Ge flux estimate and $\delta^{74/70}$Ge value of the non-opal Ge sink are highly sensitive to errors in the estimation of global hydrothermal Ge and Si fluxes. For example, at the lowest estimate of hydrothermal Si flux, the missing (non-opal) Ge sink becomes insignificant, leading to a very large uncertainty on its Ge isotope signature.

Based on this simple mass balance, our results suggest that the "missing sink" of Ge in the oceans is likely controlled by the adsorption of Ge onto Fe-oxyhydroxide in marine sediments as already proposed in previous studies (Hammond et al., 2000; King et al., 2000; McManus et al., 2003). Sulfides are also characterized by very light $\delta^{74/70}$Ge values (Escoube et al., 2012) which can potentially provide a sink for isotopically light Ge in the ocean. However, the amount of Ge sequestrated in sedimentary sulfides is probably insignificant compared to the opal and authigenic Fe oxyhydroxide sinks. This assumption is supported by the lack of Ge removal in the sulfidic and anoxic waters of the Baltic Sea (Andreae and Froelich, 1984). The importance of Ge removal with organic matter, however, will need to be further assessed considering the large Ge enrichment factors and the range of Ge isotope compositions in organic-rich rocks and compounds (Li et al., 2009; Li and Liu, 2010).

6. Synthesis and concluding remarks

In this study, we applied coupled Ge/Si and $\delta^{74/70}$Ge as new tracers in seafloor hydrothermal systems with the following systematics (**Fig. 4**):

(1) Hydrothermal fluid compositions are characterized by a high value of Ge/Si ratio and $\delta^{74/70}$Ge values, which cannot be fully explained by quartz-controlled solubility of Si in the reaction zone as the required large fractionation factor $\Delta^{74/70}Ge_{Qz\text{-}fluid}$ at about -4.1 ‰ is both unlikely and highly dependent on the Ge/Si fractionation factors (i.e. K_d values). In this study, we suggested that both quartz and sulfide precipitation in the reaction zone may control Ge/Si and Ge-isotope signatures in the fluid.

(2) Subsurface processes such as seawater-fluid mixing and conductive cooling are expected to result in contrasting Ge/Si and $\delta^{74/70}$Ge signatures of the vent fluids. In the case of simple hydrothermal fluid mixing with seawater, no variations of Ge/Si and $\delta^{74/70}$Ge are expected in the absence of Si-rich mineral precipitation. In some cases, low-temperature fluid circulation in altered basement may induce additional reactions such as: (i) enhanced fluid-rock interactions, as is the case at Pohaku vents, leading to a decrease of Ge/Si and $\delta^{74/70}$Ge toward basalt values; (ii) subsurface mineral precipitation and/or redissolution, either as sulfide or/and in Fe-oxyhydroxide and/or amorphous silica may also affect Ge/Si and Ge isotope composition in contrasting ways.

(3) Hydrothermal fluid venting at the seafloor results in extensive precipitation of a variety of Fe and Si phases, including amorphous silica, Fe oxyhydroxide and sulfides. These phases may have specific Ge isotope signatures depending on numerous parameters, such as mineralogy, temperature and attainment of isotopic equilibrium.

Finally, the heavy Ge isotope composition of hydrothermal fluids as observed at Loihi and EPR probably cannot account for the heavy Ge isotope composition of seawater, which is estimated to be 2.4 ‰ heavier compared to the average crust value. Although other major sources of Ge in seawater, such as rivers, need further investigation (e.g. Baronas et al., 2014), our finding suggests that the non-opal Ge sink in seawater is enriched in light Ge isotopes relative to seawater, which is consistent with Ge sequestration during Fe redox cycling in marine sediments, as suggested by Pokrovsky et al. (2014). Considering the growing interest of using Ge/Si and Si-isotope ratios as paleo-environmental proxies in ancient metalliferous deposits such as banded iron formations (Hamade et al., 2003; André et al., 2006; Bekker et al., 2010), Ge isotope ratios may also offer important new constrains to

determine Ge and Si sources (e.g. hydrothermal vs. continental sources) and sinks in ancient oceans.

Acknowledgements

This study was supported by the NSF (FeMO project), Europole Mer (UEB) and ANR-10-LABX-19-01. Lary Ball (WHOI), Jurek Blustajn (WHOI), Maureen Auro (WHOI), Emmanuel Ponzevera (IFREMER) and Yoan Germain (IFREMER) are thanked for their technical support. We thank the FeMO team Dave Emerson (Bigelow), Craig Moyer (WWU), Hubert Staudigel (UCSD-SIO), and Brad Tebo (OHSU) for their support and input during cruise operations. We thank the ROV *Jason-II* pilots and the crews of the R/V *Melville*, R/V *Kilo Moana*, and R/V *T. Thompson* for assistance with deployments and sample collection during the cruises. We thank Albert Galy, Alex Halliday, Philip Pogge von Strandmann, Mark Rehkämper and 3 anonymous reviewers for helpful comments and corrections on the manuscript. RE thanks Alex Halliday for a postdoctoral support (FP7) at the University of Oxford.

References

André, L., Cardinal, D., Alleman, L.Y. and Moorbath, S. (2006) Silicon isotopes in ~3.8 Ga West Greenland rocks as clues to the Eoarchaean supracrustal Si cycle. *Earth and Planetary Science Letters* **245**, 162-173.

Andreae, M.O., Froelich, P.N. (1984) Arsenic, antimony, and germanium biogeochemistry in the Baltic Sea. *Tellus Series B-Chemical and Physical Meteorology* **36**, 101-117.

Arnorsson, S. (1984) Germanium in Icelandic geothermal systems. *Geochimica et Cosmochimica Acta* **48**, 2489-2502.

Azam, F., Hemmingsen, B.B. and Volcani, B.E. (1974) Role of silicon in diatom metabolism. V. Silicic acid transport and metabolism in the heterotrophic diatom Nitzschia alba. *Archives of Microbiology* **97**, 103-114.

Azam, F. and Volcani, B.E. (1981) Germanium-silicon interactions in biological systems. *Springer-Verlag, New York*.

Bareille, G., Labracherie, M., Mortlock, R.A., Maier-Reimer, E. and Froelich, P.N. (1998) A test of (Ge/Si) opal as a paleorecorder of (Ge/Si) Seawater. *Geology* **26**, 179-182.

Baker, E.T., Embley, R.W., Walker, S.L., Resing, J.A., Lupton, J.E., Nakamura, K., de Ronde, C.E.J., Massoth, G.J. (2008). Hydrothermal activity and volcano distribution along the Mariana arc. *J. Geophys. Res.-Solid Earth* **113**, B08S09, doi:10.1029/2007JB005423.

Baronas, J.J., Hammond, D.E., McManus, J., Siebert, C., Wheat, G. (2014) Marine budget for Germanium stable isotopes. *Ocean Sciences Meeting, Honolulu, 24-28th February 2014*, Abstract ID:13978.

Bekker, A., Slack, J.F., Planavsky, N., Krapež, B., Hofmann, A., Konhauser, K.O., Rouxel, O.J. and Wing, B.A. (2010) Iron Formation: The Sedimentary Product of a Complex Interplay Among Mantle, Tectonic, and Biospheric Processes. *Economic Geology* **105**, 467-508.

Belissont, R., Boiron, M.-C., Luais, B. and Cathelineau, M. (2014) LA-ICP-MS analyses of minor and trace elements and bulk Ge isotopes in zoned Ge-rich sphalerites from the Noailhac – Saint-Salvy deposit (France): Insights into incorporation mechanisms and ore deposition processes. *Geochimica et Cosmochimica Acta* **126**, 518-540.

Bernstein, L.R. (1985) Germanium geochemistry and mineralogy. *Geochimica et Cosmochimica Acta* **49**, 2409-2422.

Butterfield, D.A., Nakamura, K., Takano, B., Lilley, M.D., Lupton, J.E., Resing, J.A., Roe, K.K. (2011) High SO2 flux, sulfur accumulation, and gas fractionation at an erupting submarine volcano. *Geology* **39**, 803-806.

Craddock, P.R., Bach, W., Seewald, J.S., Rouxel, O.J., Reeves, E., Tivey, M.K. (2010) Rare earth element abundances in hydrothermal fluids from the Manus Basin, Papua New Guinea: Indicators of sub-seafloor hydrothermal processes in back-arc basins. *Geochimica et Cosmochimica Acta* **74**, 5494-5513.

De Argollo, R. and Schilling, J.G. (1978) Ge-Si and Ga-Al fractionation in Hawaiian volcanic rocks. *Geochimica et Cosmochimica Acta* **42**, 623-630.

De Carlo, E.H., McMurtry, G.M. and Yeh, H.-W. (1983) Geochemistry of hydrothermal deposits from Loihi submarine volcano, Hawaii. *Earth and Planetary Science Letters* **66**, 438-449.

Edmond, J.M., Measures, C., McDuff, R.E., Chan, L.H., Collier, R., Grant, B., Gordon, L.I. and Corliss, J.B. (1979) Ridge crest hydrothermal activity and the balances of the major and minor elements in the ocean: The Galapagos data. *Earth and Planetary Science Letters* **46**, 1-18.

Edwards, K.J., Glazer, B.T., Rouxel, O.J., Bach, W., Emerson, D., Davis, R.E., Toner, B.M., Chan, C.S., Tebo, B.M., Staudigel, H. and Moyer, C.L. (2011) Ultra-diffuse hydrothermal venting supports Fe-oxidizing bacteria and massive umber deposition at 5000[thinsp]m off Hawaii. *ISME J* **5**, 1748-1758.

Elderfield, H. and Schultz, A. (1996) Mid-ocean ridge hydrothermal fluxes and the chemical composition of the ocean. *Annu. Rev. Earth Planet. Sci.* **24**, 191-224.

Emerson, D. and Moyer, C.L. (2002) Neutrophilic Fe-oxidizing bacteria are abundant at the Loihi Seamount hydrothermal vents and play a major role in Fe oxide deposition. *Applied and Environmental Microbiology* **68**, 3085-3093.

Emerson, D., Rentz, J.A., Lilburn, T.G., Davis, R.E., Aldrich, H., Chan, C. and Moyer, C.L. (2007) A Novel Lineage of Proteobacteria Involved in Formation of Marine Fe-Oxidizing Microbial Mat Communities. *PLoS ONE* **2**, e667.

Escoube, R., Rouxel, O.J., Luais, B., Ponzevera, E. and Donard, O.F. (2012) An Intercomparison Study of the Germanium Isotope Composition of Geological Reference Materials. *Geostandards and Geoanalytical Research* **36**, 149-159.

Evans, M.J. and Derry, L.A. (2002) Quartz control of high germanium/silicon ratios in geothermal waters. *Geology* **30**, 1019-1022.

Feely, R.A., Massoth, G.J., Baker, E.T., Cowen, J.P., Lamb, M.F., Krogslund, K.A. (1990) The effect of hydrothermal processes on midwater phosphorus distributions in the northeast Pacific. *Earth and Planetary Science Letters* **96**, 305-318.

Feely, R.A., Trefry, J.H., Massoth, G.J., Metz, S. (1991) A comparison of the scavenging of phosphorus and arsenic from seawater by hydrothermal iron oxyhydroxides in the Atlantic and Pacific Oceans. *Deep-Sea Research Part a-Oceanographic Research Papers* **38**, 617-623.

Fleming, E.J., Davis, R.E., McAllister, S.M., Chan, C.S., Moyer, C.L., Tebo, B.M. and Emerson, D. (2013) Hidden in plain sight: discovery of sheath-forming, iron-oxidizing Zetaproteobacteria at Loihi Seamount, Hawaii, USA. *Fems Microbiology Ecology* 85, 116-127.

Fornari, D.J., Shank, T., Von Damm, K.L., Gregg, T.K.P., Lilley, M., Levai, G., Bray, A., Haymon, R.M., Perfit, M.R. and Lutz, R. (1998) Time-series temperature measurements at high-temperature hydrothermal vents, East Pacific Rise 9°49'-51'N: Evidence for monitoring a crustal cracking event. *Earth and Planetary Science Letters* **160**, 419-431.

Frey, F.A. and Clague, D.A. (1983) Geochemistry of diverse basalt types from Loihi Seamount, Hawaii: petrogenetic implications. *Earth Planet. Sci. Lett.* **66**, 337–355.

Froelich, P.N. and Andreae, M.O. (1981) The marine geochemistry of germanium: Ekasilicon. *Science* **213**, 205-207.

Froelich, P.N., Blanc, V., Mortlock, R.A., Chillrud, S.N., Dunstan, W., A., U. and Peng, T.-H. (1992) River fluxes of dissolved silica to the ocean were higher during glacials: Ge/Si in diatoms, rivers, and oceans. *Paleoceanography* **7**, 739-767.

Froelich, P.N., Hambrick, G.A., Andreae, M.O., Mortlock, R.A. and Edmond, J.M. (1985a) The geochemistry of germanium in natural waters. *J. Geophys. Res.* **90**, 1133-1141.

Froelich, P.N., Hambrick, G.A., Kaul, L.W., Byrd, J.T. and Lecointe, O. (1985b) Geochemical behavior of inorganic germanium in an unperturbed estuary. *Geochimica et Cosmochimica Acta* **49**, 519-524.

Froelich, P.N., Mortlock, R.A. and Shemesh, A. (1989) Inorganic germanium and silica in the Indian Ocean: biological fractionation during (Ge/Si)Opal formation. *Global Biogeochemical Cycles* **3**, 79-88.

Glazer, B.T. and Rouxel, O.J. (2009) Redox speciation and distribution within diverse Iron-dominated microbial habitats at Loihi Seamount. *Geomicrobiology Journal* **26**, 606-622.

Haddad, A.G., Fakra, S.C., Orcutt, B.N., Toner, B.M., Chan, C.S., Rouxel, O.J. and Edwards, K.J. (in prep) Preservation of biogenic Fe oxyhydroxides in microbial mats at Loihi Seamount, Hawaii. *submitted to Geochim Cosmochim Acta.*

Halicz, L. (1985) Determination of germanium in silicate rocks and sulphide ores by hydride generation and flame atomic-absorption spectrophotometry. *The Analyst* **110**, 943-946.

Hamade, T., Konhauser, K.O., Raiswell, R., Goldsmith, S. and Morris, R.C. (2003) Using Ge/Si ratios to decouple iron and silica fluxes in Precambrian banded iron fomations. *Geology* **31**, 35-38.

Hammond, D.E., McManus, J., Berelson, W.M., Meredith, C., Klinkhammer, G.P. and Coale, K.H. (2000) Diagenetic fractionation of Ge and Si in reducing sediments: the missing Ge sink and a possible mechanism to cause glacial/interglacial variations in oceanic Ge/Si. *Geochimica et Cosmochimica Acta* **64**, 2453-2465.

Haymon, R.M., Fornari, D.J., Von Damm, K.L., Lilley, M.D., Perfit, M.R., Edmond, J.M., Shanks Iii, W.C., Lutz, R.A., Grebmeier, J.M., Carbotte, S., Wright, D., McLaughlin, E., Smith, M., Beedle, N. and Olson, E. (1993) Volcanic eruption of the mid-ocean ridge along the East Pacific Rise crest at 9°45-52'N: Direct submersible observations of seafloor phenomena associated with an eruption event in April, 1991. *Earth and Planetary Science Letters* **119**, 85-101.

John, S.G., Rouxel, O.J., Craddock, P.R., Engwall, A.M. and Boyle, E.A. (2008) Zinc stable isotopes in seafloor hydrothermal vent fluids and chimneys. *Earth and Planetary Science Letters* **269**, 17-28.

Karl, D.M., McMurtry, G.M., Malahoff, A. and Garcia, M.O. (1988) Loihi Seamount, Hawaii: A mid-plate volcano with a distinctive hydrothermal system. *Nature* **335**, 532-535.

King, S.L., Froelich, P.N. and Jahnke, R.A. (2000) Early diagenesis of germanium in sediments of the Antarctic South Atlantic: in search of the missing Ge sink. *Geochimica et Cosmochimica Acta* **64**, 1375-1390.

Kurtz, A.C., Derry, L.A. and Chadwick, O.A. (2002) Germanium-silicon fractionation in the weathering environment. *Geochimica et Cosmochimica Acta* **66**, 1525-1537.

Lewin, J.C. (1966) Silicon metabolism in diatoms. V. Germanium dioxide, a specific inhibitor of diatom growth. *Phyeologia* **6**, 1-12

Li, X., Zhao, H., Tang, M. and Liu, Y. (2009) Theoretical prediction for several important equilibrium Ge isotope fractionation factors and geological implications. *Earth and Planetary Science Letters* **287**, 1-11.

Li, X.F. and Liu, Y. (2010) First-principles study of Ge isotope fractionation during adsorption onto Fe(III)-oxyhydroxides surfaces. *Chemical Geology* **278**, 15-22.

Mantoura, S.C. (2006) Development and Application of Opal based Paleoceanographic Proxies. *Unpublished Ph.D thesis*, Univ of Cambridge, England, 218pp.

McManus, J., Hammond, D.E., Cummins, K., Klinkhammer, G.P. and Berelson, W.M. (2003) Diagenetic Ge-Si fractionation in continental margin environments: further evidence for a nonopal Ge sink. *Geochimica et Cosmochimica Acta* **67**, 4545-4557.

Mortlock, R.A. and Froelich, P.N. (1986) Hydrothermal germanium over the Southern East Pacific Rise. *Science* **231**, 43-45.

Mortlock, R.A. and Froelich, P.N. (1987) Continental weathering of germanium: Ge/Si in the global river discharge. *Geochimica et Cosmochimica Acta* **51**, 2075-2082.

Mortlock, R.A. and Froelich, P.N. (1996) Determination of germanium by isotope dilution-hydride generation inductively coupled plasma mass spectrometry. *Analytica Chimica Acta* **332**, 277-284.

Mortlock, R.A., Froelich, P.N., Feely, R.A., Massoth, G.J., Butterfield, D.A. and Lupton, J.E. (1993) Silica and germanium in Pacific Ocean hydrothermal vents and plumes. *Earth and Planetary Science Letters* **119**, 365-378.

Mottl, M.J. (1983) Metabasalts, axial hot springs, and the structure of hydrothermal systems at mid-ocean ridges. *Geological Society of America Bulletin* **94**, 161-180.

Murnane, R.J. and Stallard, R.F. (1988) Germanium/silicon fractionation during biogenic opal formation. *Paleoceanography* **3**, 461-469.

Murnane, R.J. and Stallard, R.F. (1990) Germanium and silicon in rivers of the Orinoco drainage basin. *Nature* **344**, 749-752.

Pokrovski, G.S., Roux, J., Hazemann, J.-L. and Testemale, D. (2005) An X-ray absorption spectroscopy study of argutite solubility and aqueous Ge(IV) speciation in hydrothermal fluids to 500 [degree sign]C and 400 bar. *Chemical Geology* **217**, 127-145.

Pokrovski, G.S. and Schott, J. (1998) Thermodynamic properties of aqueous Ge(IV) hydroxide complexes from 25 to 350[degree sign]C: Implications for the behavior of germanium and the Ge/Si ratio in hydrothermal fluids. *Geochimica et Cosmochimica Acta* **62**, 1631-1642.

Pokrovsky, O.S., Galy, A., Schott, J., Pokrovski, G.S. and Mantoura, S. (2014) Germanium isotope fractionation during Ge adsorption on goethite and its coprecipitation with Fe oxy(hydr)oxides. *Geochimica et Cosmochimica Acta* **131**, 138-149.

Pokrovsky, O.S., Pokrovski, G.S., Schott, J. and Galy, A. (2006) Experimental study of germanium adsorption on goethite and germanium coprecipitation with iron hydroxide: X-ray absorption fine structure and macroscopic characterization. *Geochimica et Cosmochimica Acta* **70**, 3325-3341.

Qi, H.-W., Rouxel, O., Hu, R.-Z., Bi, X.-W. and Wen, H.-J. (2011) Germanium isotopic systematics in Ge-rich coal from the Lincang Ge deposit, Yunnan, Southwestern China. *Chemical Geology* **286**, 252-265.

Resing, J.A., Lebon, G., Baker, E.T., Lupton, J.E., Embley, R.W., Massoth, G.J., Chadwick, W.W., De Ronde, C.E.J. (2007) Venting of acid-sulfate fluids in a high-sulfidation setting at NW rota-1 submarine volcano on the mariana arc. *Economic Geology* **102**: 1047-1061.

Rouxel, O., Galy, A. and Elderfield, H. (2006) Germanium isotopic variations in igneous rocks and marine sediments. *Geochimica et Cosmochimica Acta* **70**, 3387-3400.

Rouxel, O., Shanks Iii, W.C., Bach, W. and Edwards, K.J. (2008) Integrated Fe- and S-isotope study of seafloor hydrothermal vents at East Pacific Rise 9-10°N. *Chemical Geology* **252**, 214-227.

Scribner, A.M., Kurtz, A.C., Chadwick, O.A. (2006) Germanium sequestration by soil: Targeting the roles of secondary clays and Fe-oxyhydroxides. *Earth and Planetary Science Letters* **243**, 760-770.

Sedwick, P.N., McMurtry, G.M. and Macdougall, J.D. (1992) Chemistry of hydrothermal solutions from Pele's Vents, Loihi Seamount, Hawaii. *Geochimica et Cosmochimica Acta* **56**, 3643-3667.

Shank, T.M., Fornari, D.J., Von Damm, K.L., Lilley, M.D., Haymon, R.M. and Lutz, R.A. (1998) Temporal and spatial patterns of biological community development at nascent deep-sea hydrothermal vents (9°50'N, East Pacific Rise). *Deep-Sea Research Part II: Topical Studies in Oceanography* **45**, 465-515.

Shemesh, A., Mortlock, R.A. and Froelich, P.N. (1989) Late Cenozoic Ge/Si record of marine biogenic opal: implications for variations of riverine fluxes to the ocean. *Paleoceanography* **4**, 221-234.

Siebert, C., Hammond, D.E., Ross, A. and McManus, J. (2011) Erratum to C. Siebert, A. Ross and J. McManus (2006), "Germanium isotope measurements of high-temperature geothermal fluids using double-spike hydride generation MC-ICP-MS", Geochimica et Cosmochimica Acta 70, 3986–3995. *Geochimica et Cosmochimica Acta* **75**, 6267-6269.

Siebert, C., Ross, A. and McManus, J. (2006) Germanium isotope measurements of high-temperature geothermal fluids using double-spike hydride generation MC-ICP-MS. *Geochimica et Cosmochimica Acta* **70**, 3986-3995.

Stein, C.A. and Stein, S. (1994) Constraints on hydrothermal heat flux through the oceanic lithosphere from global heat flow. *Journal of Geophysical Research* **99**, 3081-3095.

Tivey, M.K. (1995) The influence of hydrothermal fluid composition and advection rates on black smoker chimney mineralogy: Insights from modeling transport and reaction. *Geochimica et Cosmochimica Acta* **59**, 1933-1949.

Toner, B.M., Berquó, T.S., Michel, F.M., Sorensen, J.V., Templeton, A.S. and Edwards, K.J. (2012) Mineralogy of iron microbial mats from Loihi Seamount. *Frontiers in Microbiology* **3**.

Von Damm, K.L. (2000) Chemistry of hydrothermal vent fluids from 9°-10°N, East Pacific Rise: "Time zero," the immediate posteruptive period. *Journal of Geophysical Research B: Solid Earth* **105**, 11203-11222.

Von Damm, K.L. (2004) Evolution of the hydrothermal system at East Pacific Rise 9′50N: geochemical evidence for changes in the upper oceanic crust. *W.S.D. Wilcock, E.F. DeLong, D.S. Kelley, J.A. Baross, S.C. Cary (Eds.), The Subsurface Biosphere at Mid-ocean Ridges, AGU Monograph* **144**

Von Damm, K.L., Bischoff, J.L. and Rosenbauer, R.J. (1991) Quartz solubility in hydrothermal seawater: an experimental study and equation describing quartz solubility for up to 0.5 M NaCl solutions. *American Journal of Science* **291**, 977-1007.

Von Damm, K.L., Edmond, J.M., Grant, B., Measures, C.I., Walden, B. and Weiss, R.F. (1985) Chemistry of submarine hydrothermal solutions at 21 °N, East Pacific Rise. *Geochimica et Cosmochimica Acta* **49**, 2197-2220.

Wheat, C.G., Jannasch, H.W., Plant, J.N., Moyer, C.L., Sansone, F.J. and McMurtry, G.M. (2000) Continuous sampling of hydrothermal fluids from Loihi Seamount after the 1996 event. *Journal of Geophysical Research B: Solid Earth* **105**, 19353-19367.

Wheat, C.G. and McManus, J. (2005) The potential role of ridge-flank hydrothermal systems on oceanic germanium and silicon balances. *Geochimica et Cosmochimica Acta* **69**, 2021-2029.

Wheat, C.G. and McManus, J. (2008) Germanium in mid-ocean ridge flank hydrothermal fluids. *Geochemistry, Geophysics, Geosystems* **9**.

Wheat, C.G., Mottl, M.J., Fisher, A.T., Kadko, D., Davis, E.E. and Baker, E. (2004) Heat flow through a basaltic outcrop on a sedimented young ridge flank. *Geochemistry, Geophysics, Geosystems* **5**.

Wheat, C.G., Mottl, M.J. and Rudnicki, M. (2002) Trace element and REE composition of a low-temperature ridge-flank hydrothermal spring. *Geochimica et Cosmochimica Acta* **66**, 3693-3705.

Figures

Fig. 1: Multibeam bathymetric map of the summit of Loihi Seamount. Contour interval corresponds to 10 m and grid size is 350 m. Active hydrothermal sites investigated in this study are shown, including Pele's Pit vents (Spillway Area: M34 and M38) and Hiolo Area (M36 and M39), Lohiau Area (M2 and M5), and Pohaku Area (M57).

Fig. 2: Chemistry of Loihi hydrothermal fluids: (a) relationship between Si (µM) and Ge (nM) for Pele's Pit vents (including Lohiau) showing a linear regression with $r^2 = 0.911$ and characterized by Ge/Si of about 31.3 µmol/mol; (b) Ge/Si versus Fe/Mn ratios showing larger variability in vent fluid composition for M57 and M5 relative to Pele's Pit vents; (c) Fe versus Mn and (d) Si versus Mn contents showing that Fe, Mn and Si concentrations are mainly controlled by dilution of the vent fluids with seawater.

Fig. 3: Ge-isotope composition ($\delta^{74/70}$Ge) of the low-temperature (21-55°C) hydrothermal fluids and Fe-rich deposits at Loihi Seamount. Data for Pele's Pit area (markers M34, M36, M38, M39), Lohiau area (markers M2 and M5) and Pohaku (marker M57) are represented with different symbols. For comparison, data for basalt and seawater are also presented. Average basalt value is from Rouxel et al. (2006) after normalization relative to NIST3120a standard as presented in Escoube et al. (2012). Seawater with a $\delta^{74/70}$Ge value of 3.0 ±0.6 ‰ has been estimated from the preliminary measurements of Baronas et al. (2014) and based on biogenic silica (Rouxel et al., 2006 and Mantoura, 2006). Error bars represent 2 sd.

Fig. 4: Schematic diagram representing the behaviour of Ge-tracers (Ge/Si and $\delta^{74/70}$Ge) in the hydrothermal system at Loihi. The diagram shows Ge/Si and $\delta^{74/70}$Ge signatures of the different hydrothermal sites investigated (Pele's Pit, Lohiau, Pohaku). This model considers the presence of a high temperature reaction zone with Ge/Si and $\delta^{74/70}$Ge signatures being similar to the high temperature (HT) hydrothermal fluid end-members measured at East Pacific Rise at 9°50'N (this study).

Tables

Table 1: Chemical and Ge isotopic composition of hydrothermal fluids at Loihi Seamount and East Pacific Rise at 9°50'N.

Table 2: Geochemical and Ge isotopic composition of Fe-rich deposits at Loihi Seamount.

Table 3: Chemical composition and sample description of mineral (mar: marcasite; py: pyrite; sph: sphalerite) separates of active and inactive sulfide deposits from East Pacific Rise (EPR) at 9-10˚N.

Table 4: Summary of Ge/Si and $\delta^{74/70}$Ge ratios measured in seafloor hydrothermal fluids.

Table 5: Determination of Ge distribution among the different phases of Fe-rich deposits at Loihi and estimation of the Ge isotope fractionation factor between Fe-oxyhydroxides (FeOOH) and hydrothermal fluid.

Table 6: Global Si and Ge fluxes in the modern ocean, and their Ge/Si and Ge isotope signatures.

Table 1: Chemical and Ge isotopic composition of hydrothermal fluids at Loihi Seamount and East Pacific Rise at 9°50'N.

Sample Name	Marker	Year	Temp	pH	Alk (a)	Ca (a)	Fe (a)	Mn (a)	Si (b)	Ge (c)	Fe/Mn	Ge/Si	$\delta^{74/70}$Ge	*2sd*
			°C		meq/kg	mM	µM	µM	µM	nM	mol/mol	µmol/mol	NIST 3120a	
Pele's Pit, Spillway Area (M34 & 38)														
J2-308-MS3-RL	M34	2007	47.0	6.72	12.8	17.1	354.7	12.3	2599	83.1	28.9	32.0	2.09	*0.11*
J2-308-MS4-RR	M34	2007	47.0	6.54	12.8	16.6	333.2	11.6	2464	81.0	28.7	32.8	2.08	*0.11*
J2-241-MS3	M34	2006	54.0	6.37	20.6	22.2	690.2	18.1	4664	152.8	38.2	32.8	1.99	*0.11*
J2-241-MS4	M34	2006	54.0	6.02	21.2	22.4	726.7	18.1	4464	177.2	40.1	39.7	1.55	*0.11*
J2-245-MS4	M34	2006	52.0	6.00	21.6	21.6	609.9	17.0	4226	151.1	35.9	35.7	1.77	*0.11*
J2-315-MS-RL	M38	2007	47.0	6.96	8.1	17.7	419.0	14.5	3096	93.4	28.8	30.2	2.20	*0.11*
J2-315-MS-RR	M38	2007	47.0			16.6	426.6	15.2	3129	96.3	28.1	30.8	1.97	*0.11*
J2-314-MS-RL	M38	2007	55.0	6.21	12.3	16.0	303.9	10.6	2360	73.3	28.6	31.1	2.17	*0.11*
J2-314-MS-RR	M38	2007	55.0	6.10	10.2	14.7	234.2	8.1	1840	54.6	28.8	29.7	1.89	*0.11*

Pele's Pit, Hiolo area (M36 & 39)														
J2-314-MS-BL	M36	2007	50.0	6.29	10.2	15.1	338.1	15.3	2604	74.6	22.1	28.7	1.50	*0.11*
J2-314-MS-BR	M36	2007	50.0	5.84	11.7	15.6	397.6	17.8	3006	88.9	22.4	29.6	1.77	*0.11*
J2-241-MS1	M36	2006	51.0	6.01	12.9	17.4	557.8	23.4	2782	113.5	23.9	40.8	1.35	*0.11*
J2-242-MS2	M36	2006	51.0	5.76	12.9	17.6	552.3	23.8	2966	82.4	23.2	27.8	1.07	*0.11*
J2-308-MS1-BL	M39	2007	45.0	6.67	14.7	18.7	576.0	24.1	4069	116.0	23.9	28.5	1.60	*0.11*
J2-308-MS2-BR	M39	2007	45.0	6.69	14.8	18.7	577.8	24.5	4131	119.5	23.6	28.9	1.74	*0.11*
J2-311-MS-BL	M39	2007	47.4	6.29	8.1	13.9	261.4	11.5	1772	48.1	22.8	27.2	1.39	*0.11*
J2-311-MS-BR	M39	2007	47.4	6.21	13.7	17.2	553.7	23.4	3591	102.4	23.7	28.5	1.21	*0.11*
J2-315-MS-BL	M39	2007	52.0	6.08	15.6	18.1	556.4	23.7	4010	118.0	23.5	29.4	1.91	*0.11*
J2-242-MS3	M39	2006	51.0	5.88	15.0	18.6	568.8	22.2	3830	118.9	25.6	31.0	1.54	*0.11*
J2-242-MS4	M39	2006	51.0	5.94	15.0	18.2	558.6	22.1	3679	129.8	25.3	35.3	1.19	*0.11*
J2-245-MS2	M39	2006	50.0	5.77	15.0	18.2	584.1	23.0	3757	115.0	25.4	30.6	1.21	*0.11*
Pele's											**27.**	**31.4**	**1.68**	***0.***

pit vents - average											**21**	**8**		***70***
Lohiau Area (M5)														
J2-311-MS-RL	M5	2007	24.5	6.94	5.6	12.9	68.3	10.0	675	34.9	6.8	51.8	1.15	*0.11*
J2-311-MS-RR	M5	2007	24.5	6.65	6.6	12.6	58.0	8.0	628	15.0	7.2	23.9	1.23	*0.11*
J2-242-MS1	M5	2006	21.0	6.21	3.4	11.5	57.7	2.8	369	14.2	20.4	38.5	0.95	*0.11*
J2-245-MS1	M5	2006	22.0	5.89	9.3	16.5	234.7	21.8	1558	32.7	10.8	21.0	1.20	*0.11*
Lohiau area - average											**11.30**	**33.80**	**1.13**	***0.25***
Pohaku area (M57)														
J2-368-MS-black	M57	2008	28.3	6.52		10.7	507.2	12.4	1553	10.1	40.9	6.5	0.61	*0.11*
J2-368-MS-red	M57	2008	26.7	5.59		11.4	773.4	19.0	2275	21.2	40.7	9.3	0.74	*0.11*
Pohaku area - average											**40.81**	**7.92**	**0.67**	***0.18***
East Pacific Rise (9°50'N)														
ALV-4057-W1	Bio 9″	2004	383.0	3.21		11.9	3173.0	483.0	11080	103.3	6.6	8.1	1.46	*0.11*
ALV-4057-	Bio 9″	2004	383.0	3.3		11.	3088.0	461.	1108	75.5	6.7	8.1	1.68	*0.1*

W2				0		9		0	0					*1*
ALV-4059-W1	Tica Vent	2004	344.0	3.16		11.5	1417.0	377.0	13105	51.1	3.8	3.7	1.23	*0.11*
ALV-4059-W2	Tica Vent	2004	344.0	3.13		11.1	1381.0	369.0	13105	46.4	3.7	3.7	1.54	*0.11*
ALV-4061-W3	Bio vent	2004	331.0	4.45		10.1	156.0	101.0	14855	79.4	1.5	6.8	1.71	*0.11*
ALV-4061-W4	Bio vent	2004	331.0	3.79		9.5	265.0	180.0	14855	115.1	1.5	6.8	1.65	*0.11*
East Pacific Rise (9°50' N) - average											**3.96**	**6.20**	**1.55**	***0.36***
Average igneous crust (d)											2.40	0.56	*0.08*	
Background seawater (e)		2.0	8.30		10.3	<0.001	<0.005	75	0.10		0.72	3.00	*0.60*	

(a) Chemical data for Loihi Seamount and EPR 9°50'N are from Glazer et al. (2009) and Rouxel et al. (2008) respectively. Alk: total alkalinity in meq/kg determined by titration.

(b) Si concentration at EPR 9-10°N determined by ICP-AES (Si data for Loihi are from Glazer and Rouxel, 2009)
(c) Ge concentration determined by isotope dillution and HG-MC-ICPMS analysis, this study

(d) Estimation of average $\delta^{74/70}$Ge of the igneous crust is from Rouxel et al. (2006) and normalized relative to NIST3120a standard in Escoube et al. (2012)
(e) Estimation of seawater $\delta^{74/70}$Ge value based on the analysis of marine biogenic opal (Rouxel et al., 2006, Mantoura et al., 2006) after renormalization to NIST3120a (Escoube et al., 2012) and preliminary seawater analysis reported by Baronas et al.

(2014). Other data data were obtained on background seawater sample recovered above Loihi Seamount

Table 2: Geochemical and Ge isotopic composition of Fe-rich deposits at Loihi Seamount

Sample Name	Marker	Year	Si (wt%)	Al (wt%)	Fe (wt%)	P (µg/g)	Ge (µg/g)	Ge/Si (µmol/mol)	$\delta^{74/70}$Ge NIST3120a	*2sd*
Pele's Pit, Hiolo area										
J2-245-SS1	M36	2006	9.58	2.31	29.11	9518	9.2	37.5	-0.08	*0.20*
duplicate									-0.10	*0.20*
J2-245-SS4	M36	2006	7.70	1.84	27.21	13841	8.6	43.3	-0.06	*0.20*
J2-242-SS4	M39	2006	5.19	0.13	38.37	8645	16.5	123.4	-0.23	*0.20*
duplicate									-0.34	*0.13*
J2-308-SS1	M39	2007	9.03	1.24	26.89	7466	18.0	77.6	-0.61	*0.13*
Pele's Pit, Spillway area										
J2-245-SS5	M34	2006	9.38	0.33	33.23	8820	23.5	97.5	-0.28	*0.20*
duplicate									-0.26	*0.13*
J2-308-SS2	M34	2007	15.51	0.69	24.36	6549	23.1	58.0	-0.66	*0.13*
J2-314-SSA/B	M34/38	2007	6.73	0.76	31.90	10173	20.5	118.1	0.16	*0.13*
Lohiau area										
J2-311-SS1	M2	2007	10.07	1.65	28.19	6244	26.5	102.3	-0.98	*0.13*
J2-245-SS3	M5	2006	7.28	0.41	34.70	6375	27.6	147.6	-0.75	*0.20*
duplicate									-0.67	*0.13*
J2-242-SS2	M5	2006	6.06	0.04	40.37	5196	29.5	189.4	-0.41	*0.13*
J2-310-SS2	M5	2007	7.42	0.33	34.57	6287	28.8	150.7	-0.69	*0.13*
Pohaku area										
J2-316-SS1	M57	2007	2.50	0.06	41.10	11134	4.8	74.4	-0.21	*0.13*
Average					1.00	2.20	0.56	*0.08*		

igneous crust (a)										

(a) Estimation of the igneous crust is from Rouxel et al. (2006) and normalized relative to NIST3120a standard as described in Escoube et al. (2012)

Table 3: Chemical composition and sample description of mineral separates of active and inactive sulfide deposits from East Pacific Rise (EPR) at 9˚50'N

Sample Name	minerals (a)	Fe (wt%)	Cu (wt%)	Zn (wt%)	Ca (wt%)	Pb (wt%)	Ge (µg/g)	$\delta^{74/70}$Ge NIST3120a	*2sd*
Bio 9" (Cu-rich chimneys)									
ALV-4057-M1 #A1	sph-py	26.35	0.59	22.67	0.02	0.07	8.22	-3.71	*0.18*
ALV-4057-M1 #A3	sph-py	26.33	1.88	23.98	0.09	0.06	4.73	-3.82	*0.18*
ALV-4057-M1 #A4	sph-py	21.13	2.32	26.51	0.03	0.06	11.00	-4.08	*0.18*
ALV-4057-M1 #A5	sph-py	25.51	0.64	22.90	0.03	0.06	7.14	-4.37	*0.18*
Fe-Zn-rich inactive chimneys									
ALV-4053-M3	sph-py	16.03	0.40	28.44	0.01	0.73	27.37	-3.60	*0.18*
ALV-4057-M2	sph-py-mar	16.20	0.32	37.76	0.11	0.03	13.19	-4.02	*0.18*
ALV-4059-M3	sph	9.79	0.38	45.38	0.03	0.02	10.34	-4.71	*0.18*

Fe, Cu Zn, Ca and Pb determined by ICP-AES (detection limit 0.01%); Ge concentration and isotope ration determined by HG-ICPMS following the method described in Rouxel et al. (2006)
(a) mar: marcasite; py: pyrite; sph: sphalerite. Additional description of the samples is available in Rouxel et al. (2008)

Table 4: Summary of Ge/Si and $\delta^{74/70}$Ge ratios measured in seafloor hydrothermal fluids

Site (*)	Sample type	Temp (°C)	Si (µM)	Ge/Si (µmol/mol)	*2sd*	$\delta^{74/70}$Ge (‰)	*2sd*	data source
	Average igneous rock			2.4		0.56	*0.09*	(a)
	Seawater estimate	2	180	0.7		3.00	*0.60*	(b)
Loihi	Pele's Pit area	47	4664	31.5	*7.3*	1.68	*0.70*	(c)
Loihi	Lohiau area	23	1558	33.8	*28.5*	1.13	*0.25*	(c)
Loihi	Pohaku area	27	2275	7.9	*4.0*	0.67	*0.18*	(c)
EPR	9°50'N area	353	20000	6.2	*4.0*	1.55	*0.36*	(c)
EPR	21°N area	HT	16519	8.7	*3.4*			(d)
JdFR	North Cleft area	HT	22000	9.5	*7.0*			(d)
Axial Volcano	Axial Volcano	HT	12500	10.8	*1.7*			(d)
Axial Volcano	Inferno area	HT	71175	13.6	*3.1*			(d)
JdFR	Cleft segment	HT	22250	10.7	*5.3*			(d)
JdFR	Baby Bare	63	360	34.0				(e)
JdFR	ODP Hole 1025	40.5	580	15.0				(e)
JdFR	ODP Hole 1026	63	710	27.0				(e)
JdFR	ODP Hole 1027	63	320	62.0				(e)
JdFR	ODP Hole 1024	23	50	17.0				(e)
EPR	Dorado outcrop	7	180	1.7				(e)
EPR	14°S	3	170	0.7				(e)

(*) EPR: East Pacific Rise; JdFR: Juan de Fuca Ridge
(a) Estimation of average $\delta^{74/70}$Ge of the igneous crust is from Rouxel et al. (2006) and normalized relative to NIST3120a standard (Escoube et al., 2012)
(b) Estimation of $\delta^{74/70}$Ge seawater value based on the analysis of marine biogenic opal (Rouxel et al., 2006, Mantoura et al., 2006) after renormalization to NIST3120a standard
(c) This study; average values calculated from data reported in Table 1
(d) Average values of high-temperature (HT) hydrothermal vents from Mortlock et Froelich (1993)
(e) Individual data of warm and cold basaltic formation fluids from ridge flank hydrothermal systems, from Wheat and McManus (2008)

Table 5: Determination of Ge distribution among the different phases of Fe-rich deposits at Loihi and estimation of the Ge isotope fractionation factor between FeOOH and hydrothermal fluid.

Sample Name	Marker	XGe Bas (a)	*2sd*	XGe Amo (a)	*2sd*	XGe FeOOH (a)	*2sd*	$\delta^{74/70}$ Ge bulk (b)	*2sd*	$\delta^{74/70}$ Ge FeOOH	*2sd*	$\Delta^{74/70}$ Ge FeOOH-Fluid (c)	*2sd*	f_{ads}
Pele's Pit, Hiolo area														
J2-245-SS1	M36	0.04	*<0.01*	0.11	*0.10*	0.85	*0.10*	-0.08	*0.20*	-0.33	*0.37*	-1.89	*0.77*	0.37
J2-245-SS4	M36	0.03	*<0.01*	0.10	*0.09*	0.87	*0.09*	-0.06	*0.20*	-0.26	*0.22*	-1.65	*0.69*	0.45
J2-242-SS4	M39	*<0.01*	*<0.01*	0.10	*0.10*	0.90	*0.10*	-0.23	*0.20*	-0.44	*0.31*	-1.98	*0.59*	0.34
J2-308-SS1	M39	0.01	*<0.01*	0.11	*0.05*	0.88	*0.05*	-0.61	*0.13*	-0.85	*0.24*	-2.29	*0.65*	0.24
Pele's Pit, Spillway area														
J2-245-SS5	M34	*<0.01*	*<0.01*	0.15	*0.11*	0.84	*0.11*	-0.28	*0.20*	-0.65	*0.36*	-2.50	*0.57*	0.17
J2-308-SS2	M34	*<0.01*	*<0.01*	0.27	*0.17*	0.73	*0.17*	-0.66	*0.13*	-1.63	*0.85*	-3.55	*0.95*	0.00
J2-314-SSA/B	M34/38	0.01	*<0.01*	0.09	*0.07*	0.91	*0.07*	0.16	*0.13*	-0.03	*0.25*	-1.92	*0.68*	0.36
Lohiau area														
J2-311-SS1	M2	0.01	*<0.01*	0.08	*0.08*	0.91	*0.08*	-0.98	*0.13*	-1.20	*0.26*	-2.34	*0.32*	0.22
J2-242-SS2	M5	*<0.01*	*<0.01*	0.10	*0.12*	0.90	*0.12*	-0.41	*0.13*	-0.58	*0.27*	-1.76	*0.42*	0.41
J2-245-SS3	M5	*<0.01*	*<0.01*	0.11	*0.14*	0.88	*0.14*	-0.75	*0.20*	-1.04	*0.42*	-2.20	*0.52*	0.27
J2-310-SS2	M5	*<0.01*	*<0.01*	0.11	*0.13*	0.88	*0.13*	-0.69	*0.13*	-0.95	*0.40*	-2.08	*0.60*	0.31

Pohaku area													
J2-316-SS1	M57	0.00	*0.00*	0.04	*0.04*	0.96	*0.04*	-0.21	*0.13*	-0.20	*0.13*	-0.87	*0.19*	0.71

(a) XGe Bas, XGe Amo, XGe FeOOH: fraction of Ge hosted in basalt, amorphous silica and Fe-oxyhydroxide respectiviely
(b) Ge isotope composition of bulk Fe-rich deposit, from Table 2
(c) Ge isotope fractionation factor: $\Delta^{74/70}Ge_{(FeOOH-Fluid)} = \delta^{74/70}GeFeOOH - \delta^{74/70}Ge_{Fluid}$; with fluid values from Table 1
(d) fraction of Ge adsorbed onto Fe-oxyhydroxide, considering an equilibrium Ge isotope fractionation factor α between FeOOH and Fluid of 0.997. $f_{ads} = 1-\Delta^{74/70}Ge_{(FeOOH-Fluid)}/(1000*Ln(\alpha))$
2sd: 2 standard deviation determined through error propagation (Monte Carlo method)

Table 6: Global Si and Ge fluxes in modern ocean, and their Ge/Si and Ge isotope signatures.

Sources/Sinks	Si Flux	*err*	Ge Flux	*err*	Ge/Si	*err*	$\delta^{74/70}$Ge	*err*	$\Delta^{74/70}Ge_{SW-Sink}$
	(10^{12} mol/y)		(10^{6} mol/y)		(µmol/mol)		NIST3120a		(b)
Input									
Riverine (case 1)	5.60	*0.60*	3.02	*0.60*	0.54	*0.10*	0.56	*0.20*	
Riverine (case 2)	5.60	*0.60*	3.02	*0.60*	0.54	*0.10*	3.00	*0.20*	
Eolian	0.50	*0.50*	0.27	*0.30*	0.54		0.56	*0.20*	
Hydrothermal	0.55	*0.10*	6.05	*1.08*	11.00	*3.00*	1.55	*0.36*	
LT basalt + flanks	0.82	*0.41*	1.10	*0.55*	1.34	*0.67*	1.20	*0.50*	
Output									
Opal burial (a)	7.47	*0.89*	5.23	*0.63*	0.70	*0.10*	3.00	*0.20*	
Non-opal sink (case 1)	0.00		5.22	*1.52*			-0.58	*0.60*	3.58
Non-opal sink (case 2)	0.00		5.22	*1.52*			0.87	*0.40*	2.13

See text for discussion and appropriate references relative to the assigned values
"err" corresponds to the estimated uncertainty of both input or output values used in the box model
(a) Opal burial sink is determined by assuming no Ge/Si and Ge isotope fractionation relative to seawater

case 1 assumes a global riverine flux with Ge isotope composition identical to bulk crust values
case 2 assumes a global riverine flux with Ge isotope composition identical to seawater
(b) Signature of the missing sink for the case 1 and case 2 corresponding to the difference between seawater and Non-opal sink Ge composition

Figure 1

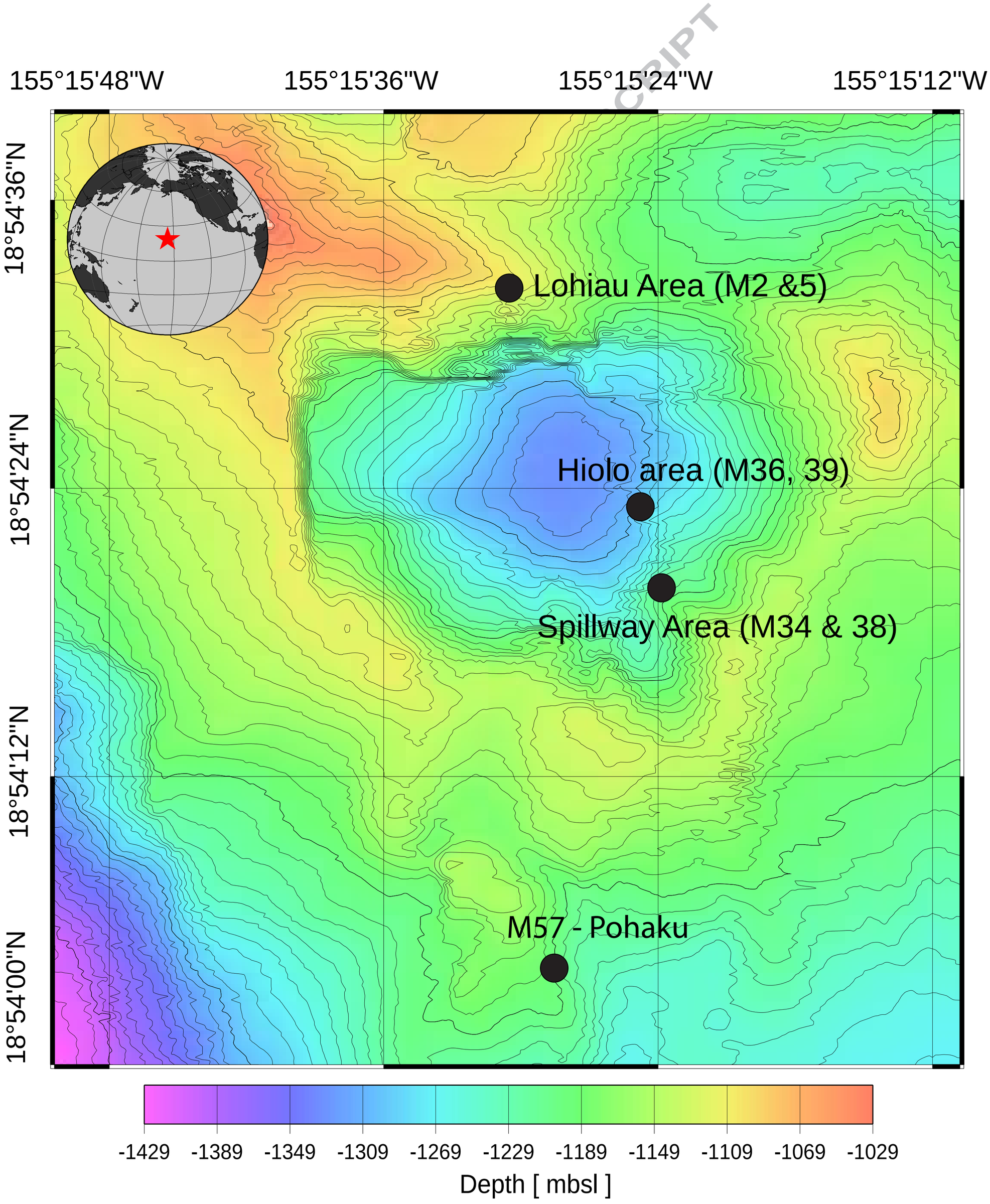

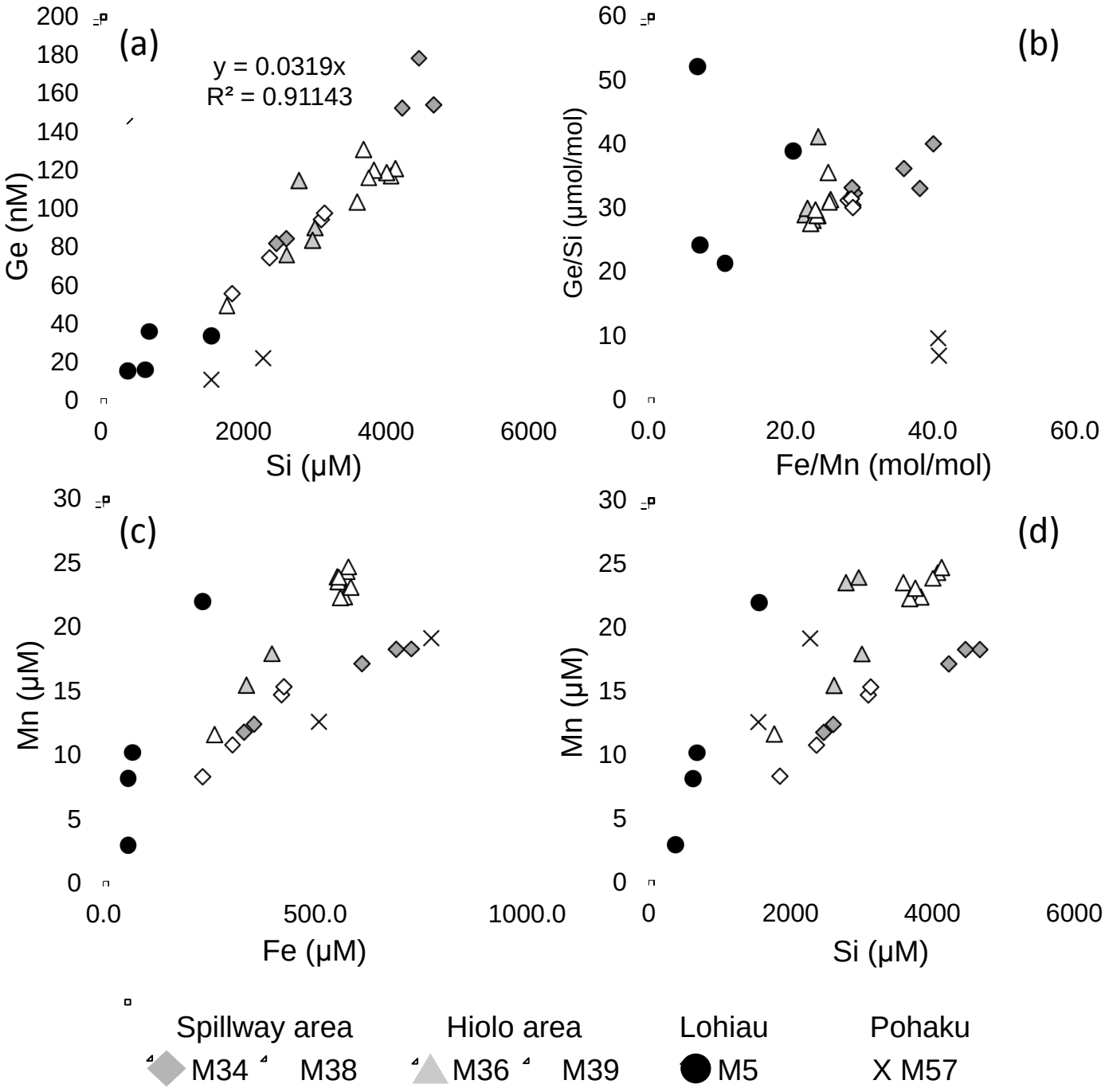

Figure 2

Figure 3

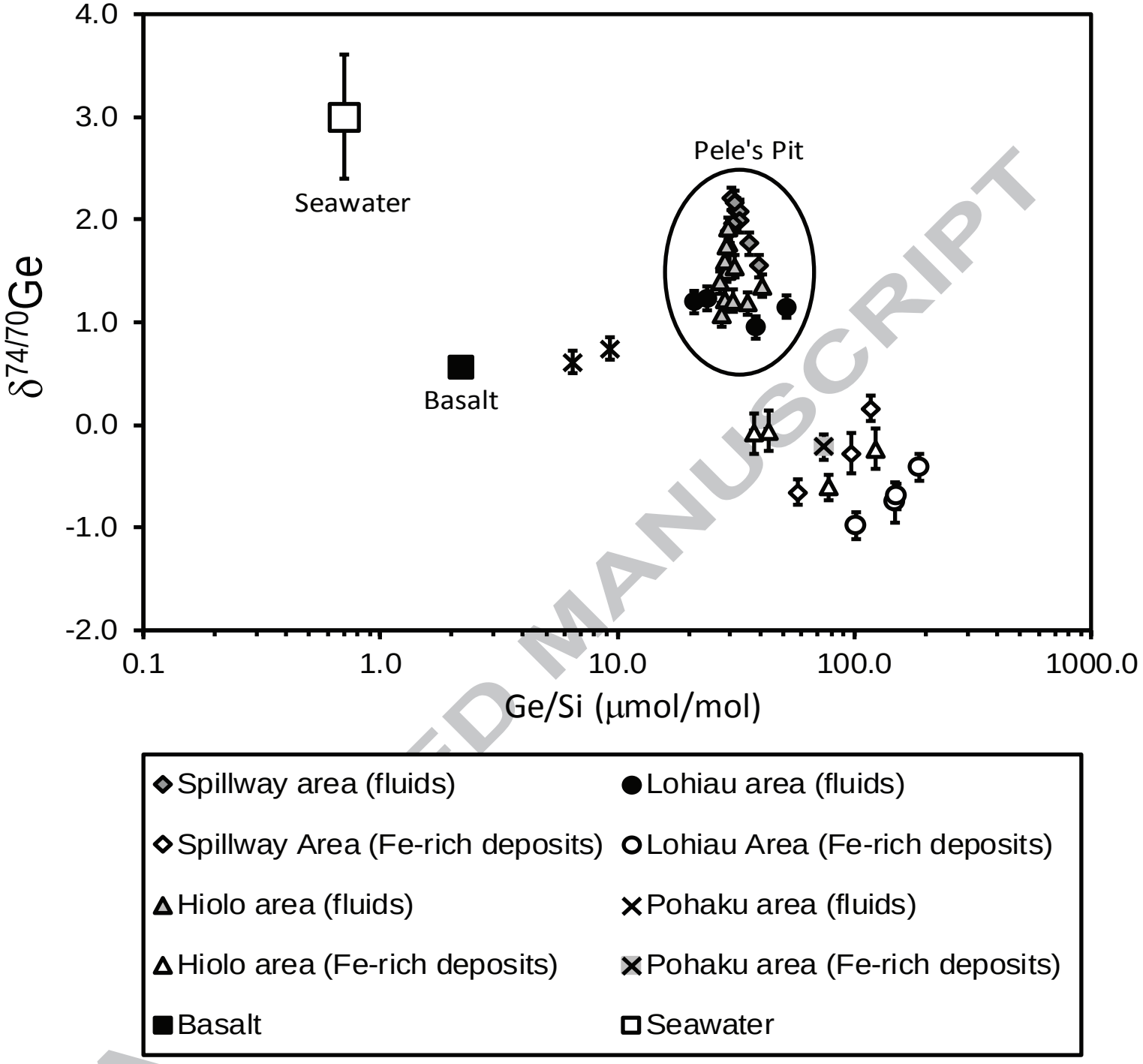

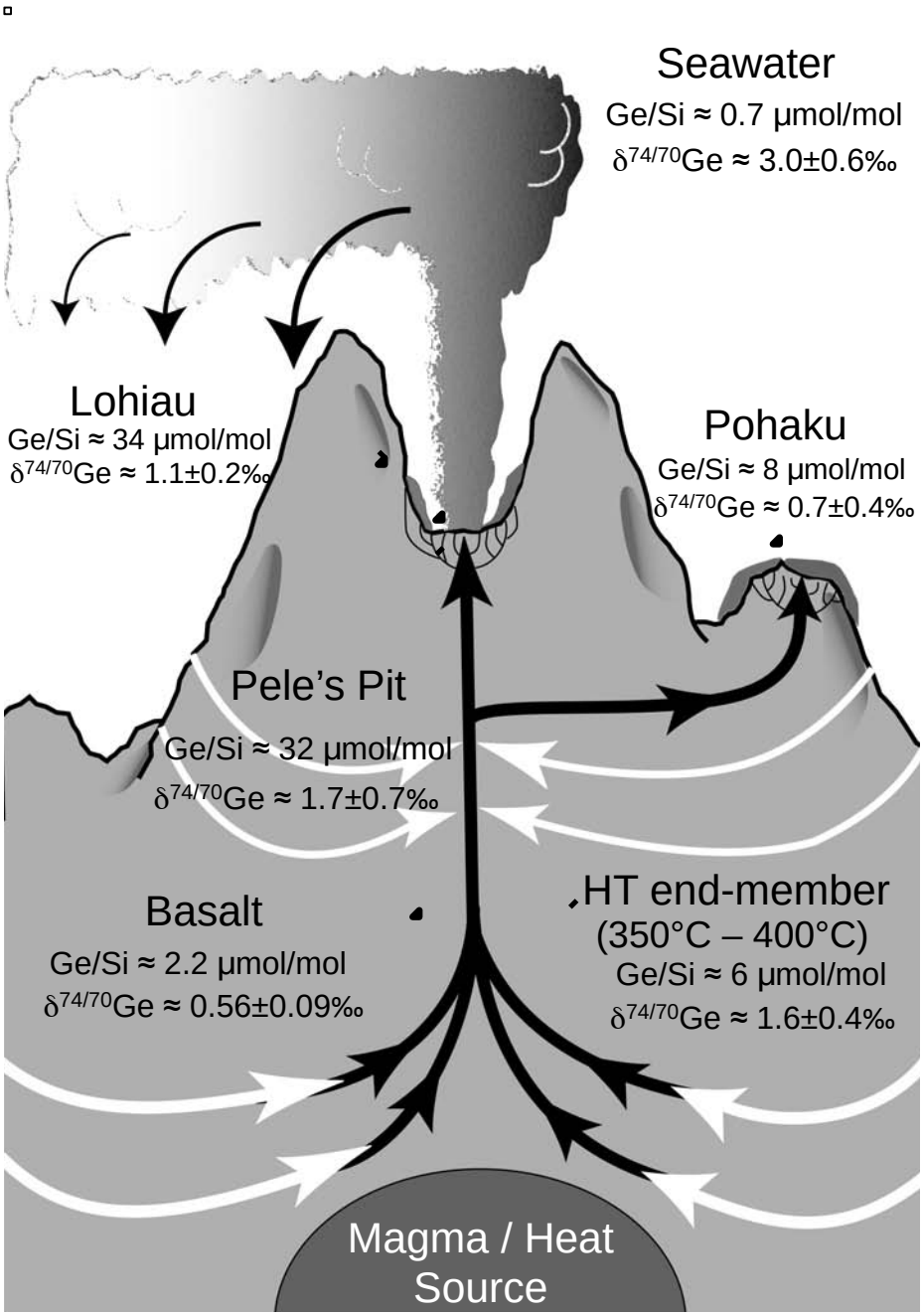

Figure 4